Did LIGO detect Primordial Black Holes?

EPTA
PPTA
NANOGrav
IPTA
FAST
SKA

LISA
Taiji
TianQin

LIGO
Virgo
KAGRA

Qing-Guo Huang

Institute of theoretical physics, CAS
National Astronomical Observatories, CAS

20/10/2021

General Relativity

$$R_{\mu\nu} - \frac{1}{2}Rg_{\mu\nu} = 8\pi G T_{\mu\nu}$$

$$r_{BH} = 2GM$$

Gravitational Waves

$$g_{\mu\nu} = \eta_{\mu\nu} + h_{\mu\nu}, \quad \Box h_{\mu\nu} = 0$$

$$t_{\mu\nu} = \frac{1}{32\pi G}\langle \partial_\mu h^{TT}_{\rho\sigma} \partial_\nu h^{\rho\sigma}_{TT} \rangle$$

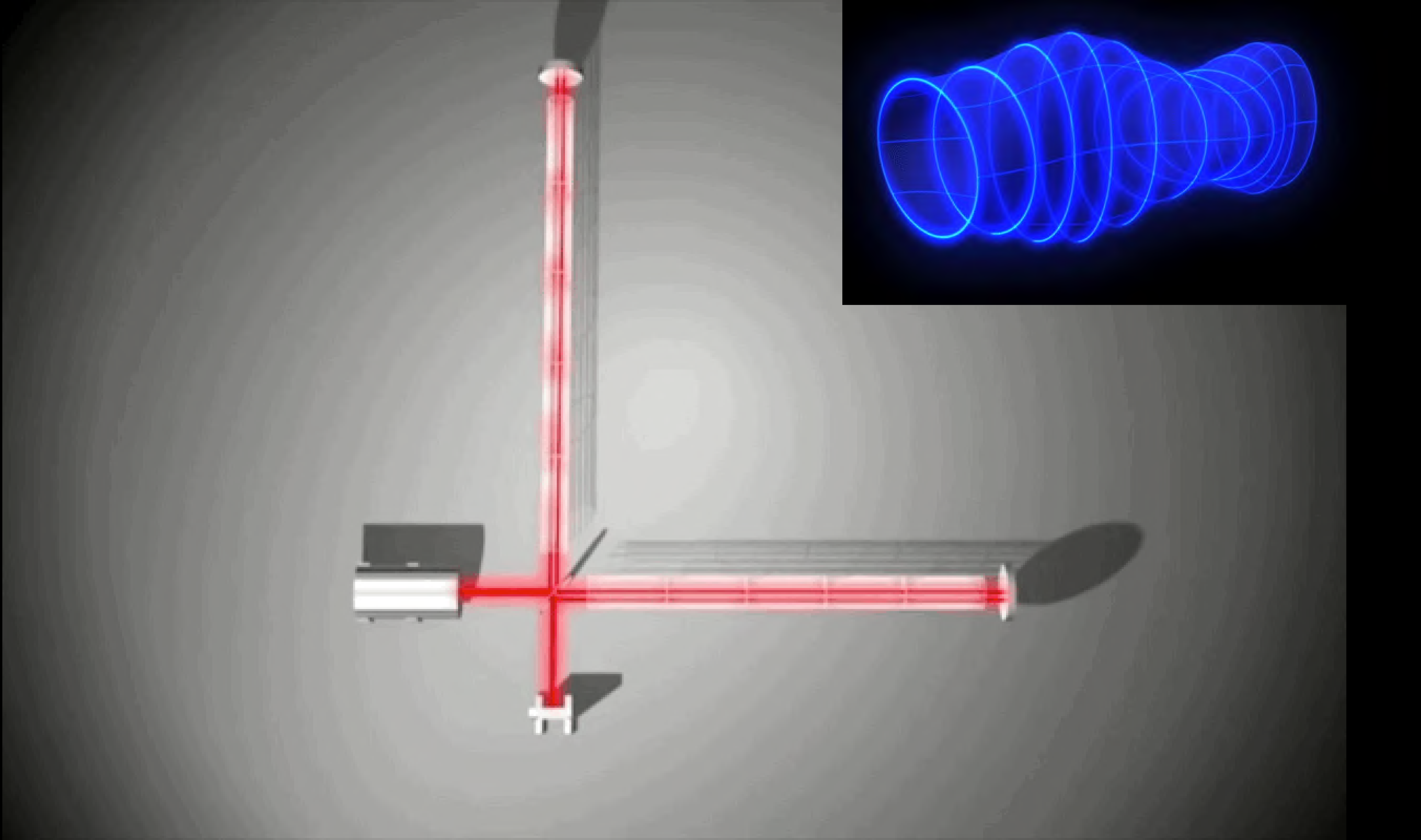

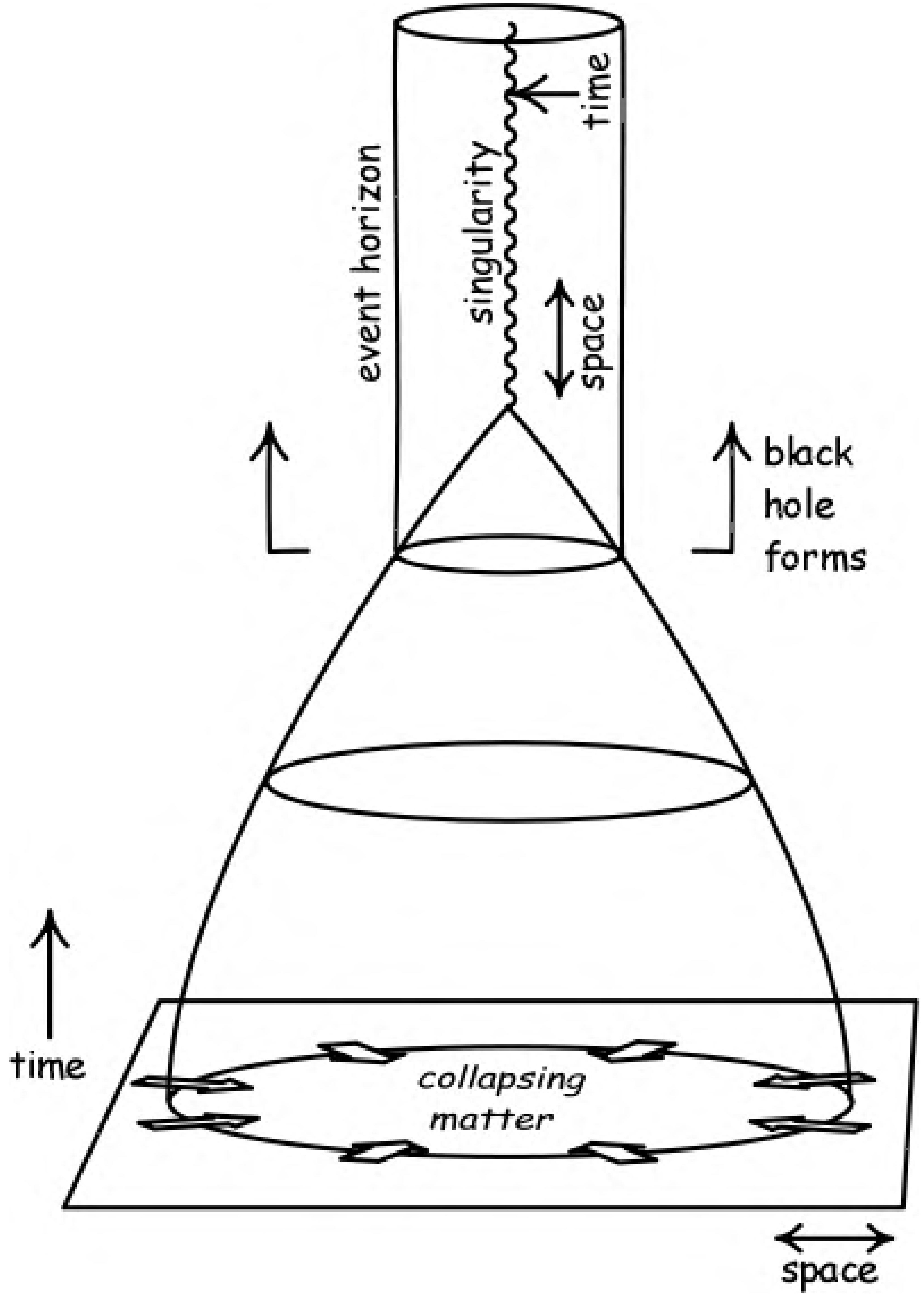

time
event horizon
singularity
space
black
hole
forms
time
collapsing
matter
space

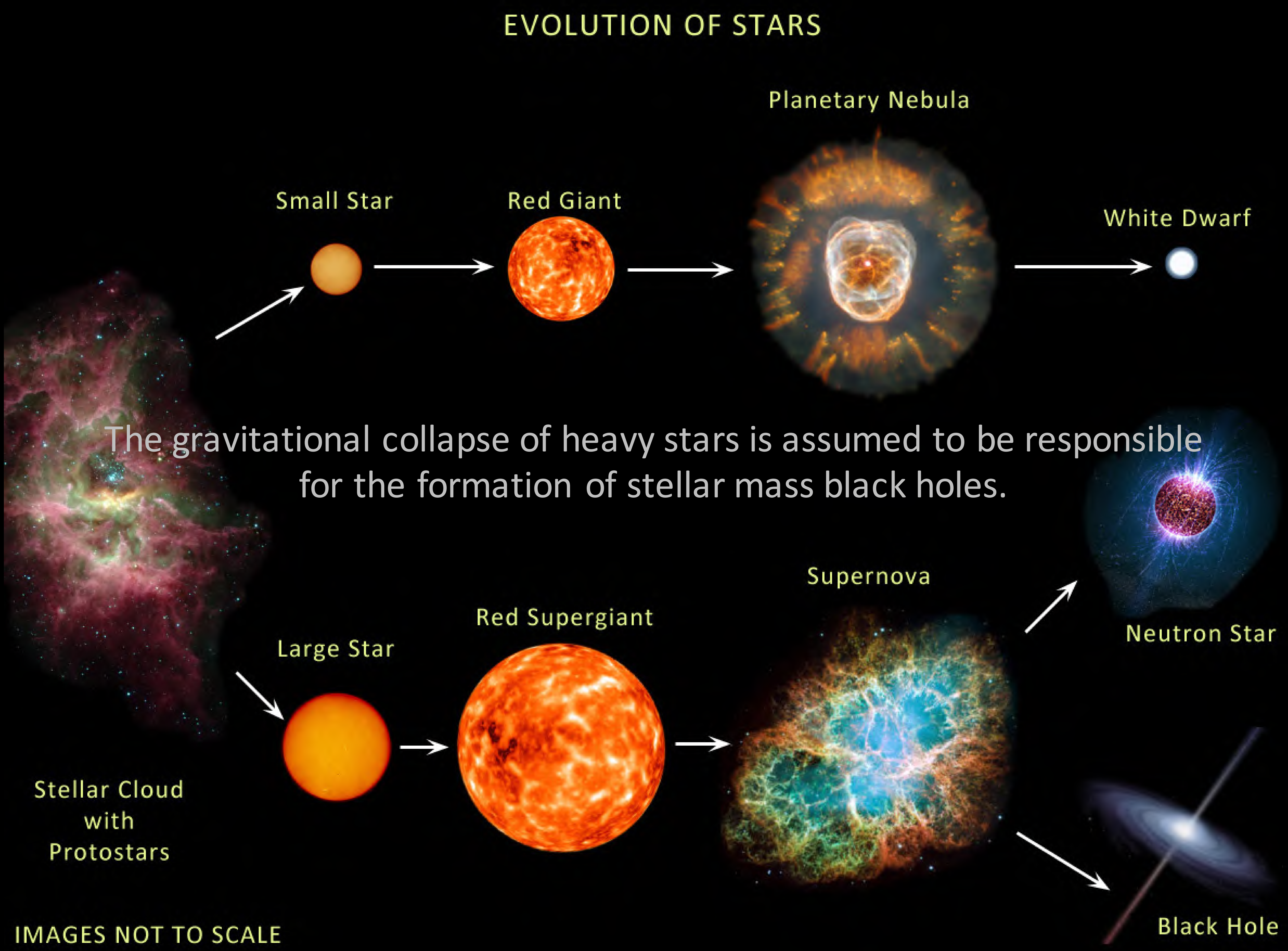

The gravitational collapse of heavy stars is assumed to be responsible for the formation of stellar mass black holes.

Density Perturbations and formation of PBHs

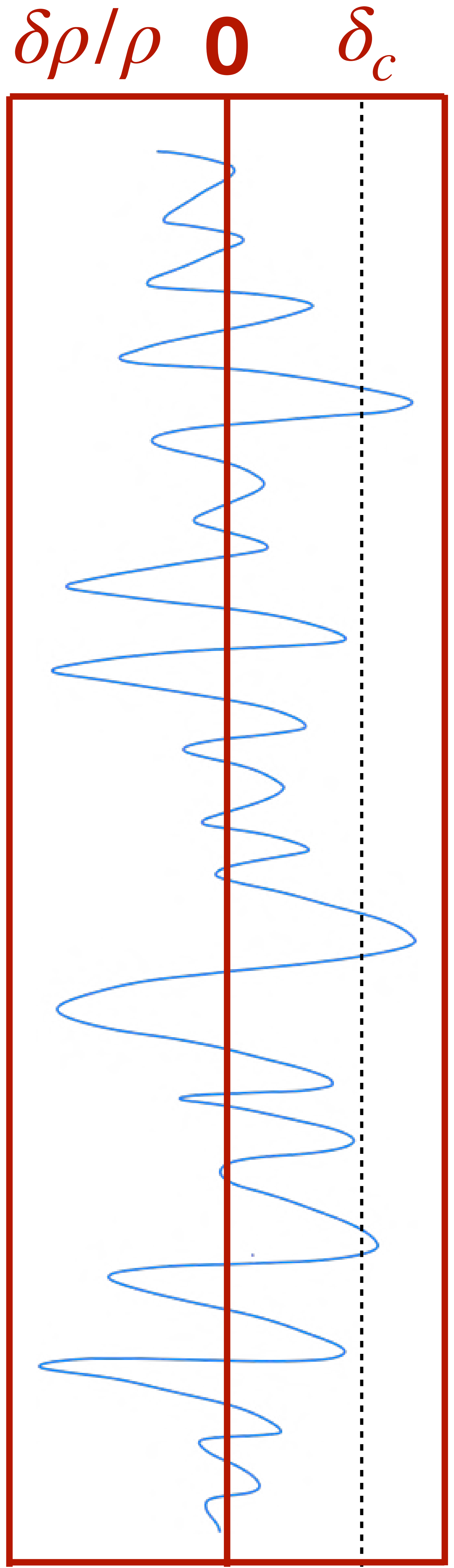

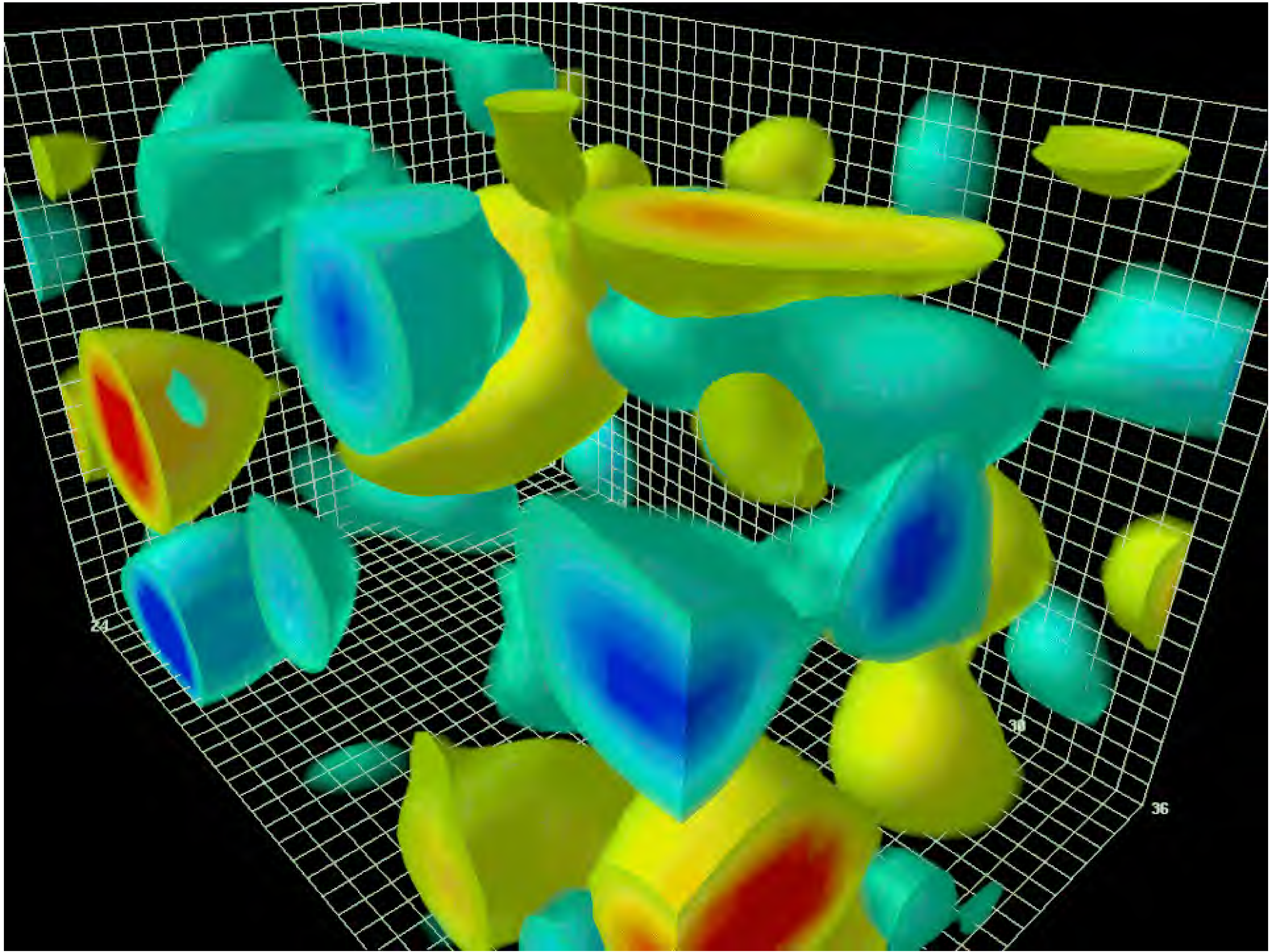

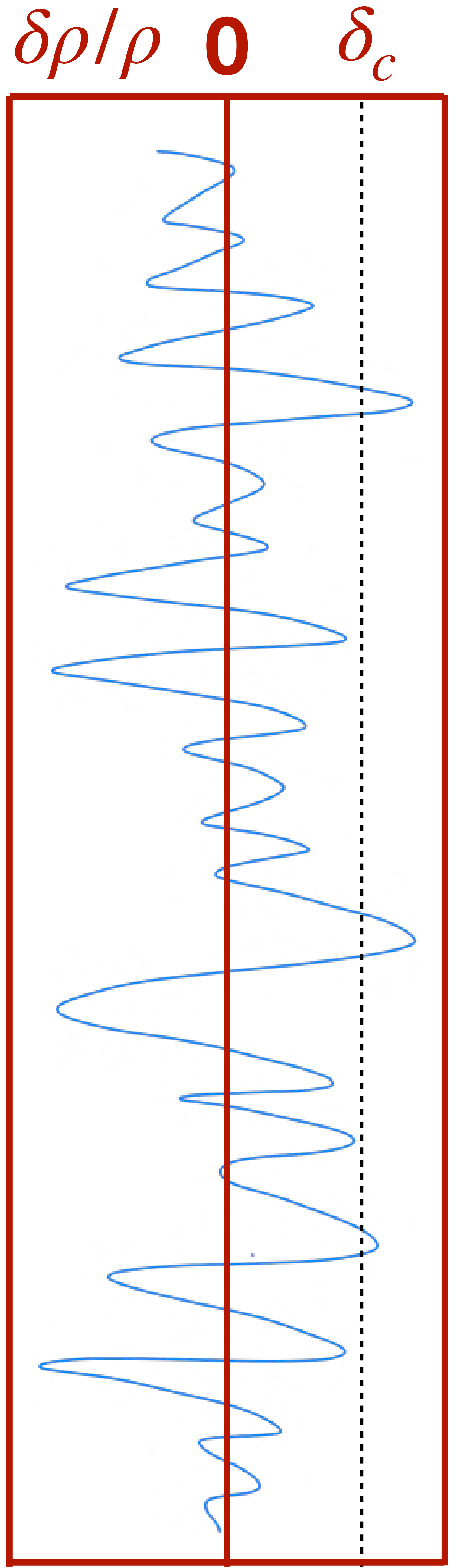

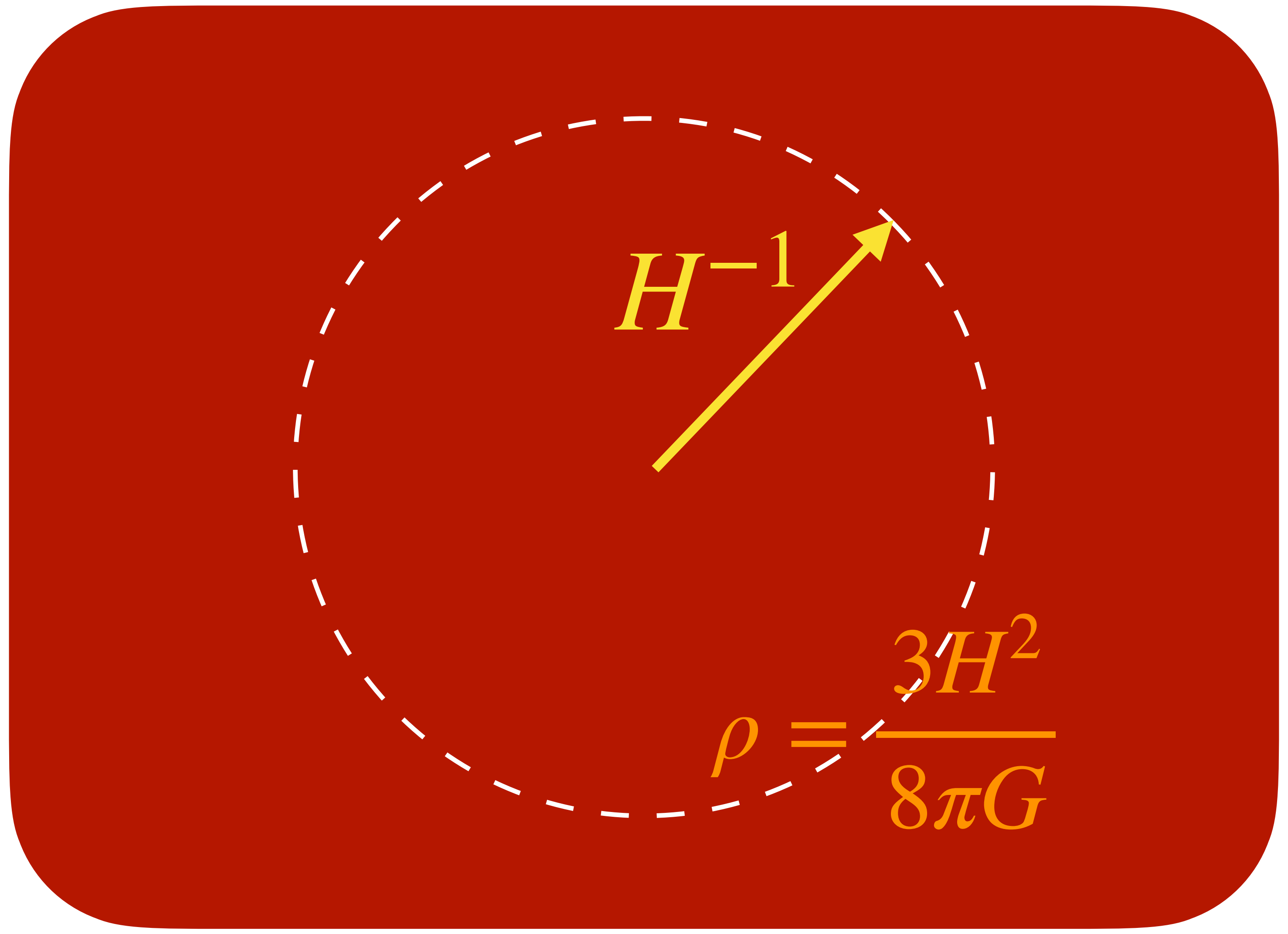

$$E = \rho \times \frac{4\pi}{3}\left(H^{-1}\right)^3 = \frac{H^{-1}}{2G}$$

$$2GE = H^{-1}$$

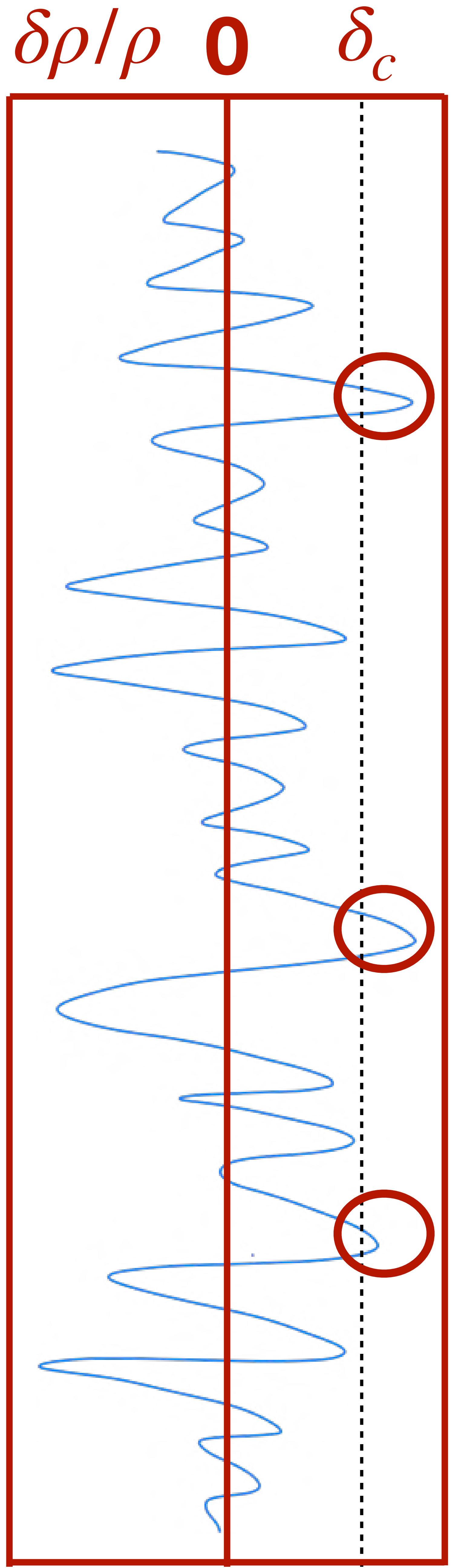

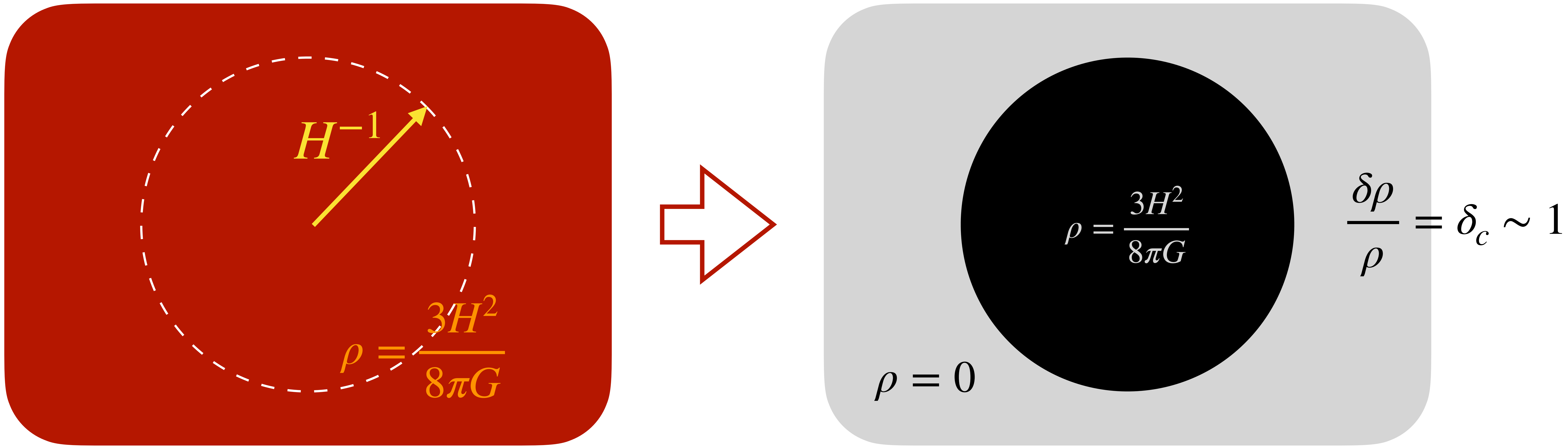

$$E = \rho \times \frac{4\pi}{3} \left(H^{-1}\right)^3 = \frac{H^{-1}}{2G}$$

$$2GE = H^{-1}$$

Primordial Black Hole (PBH)

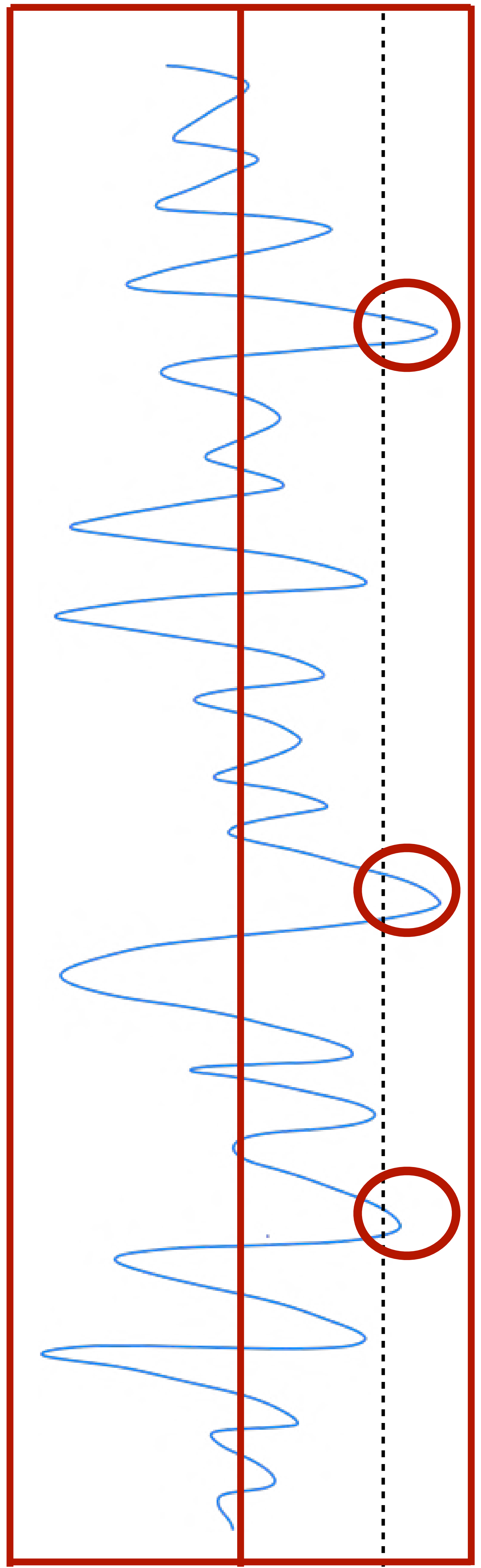

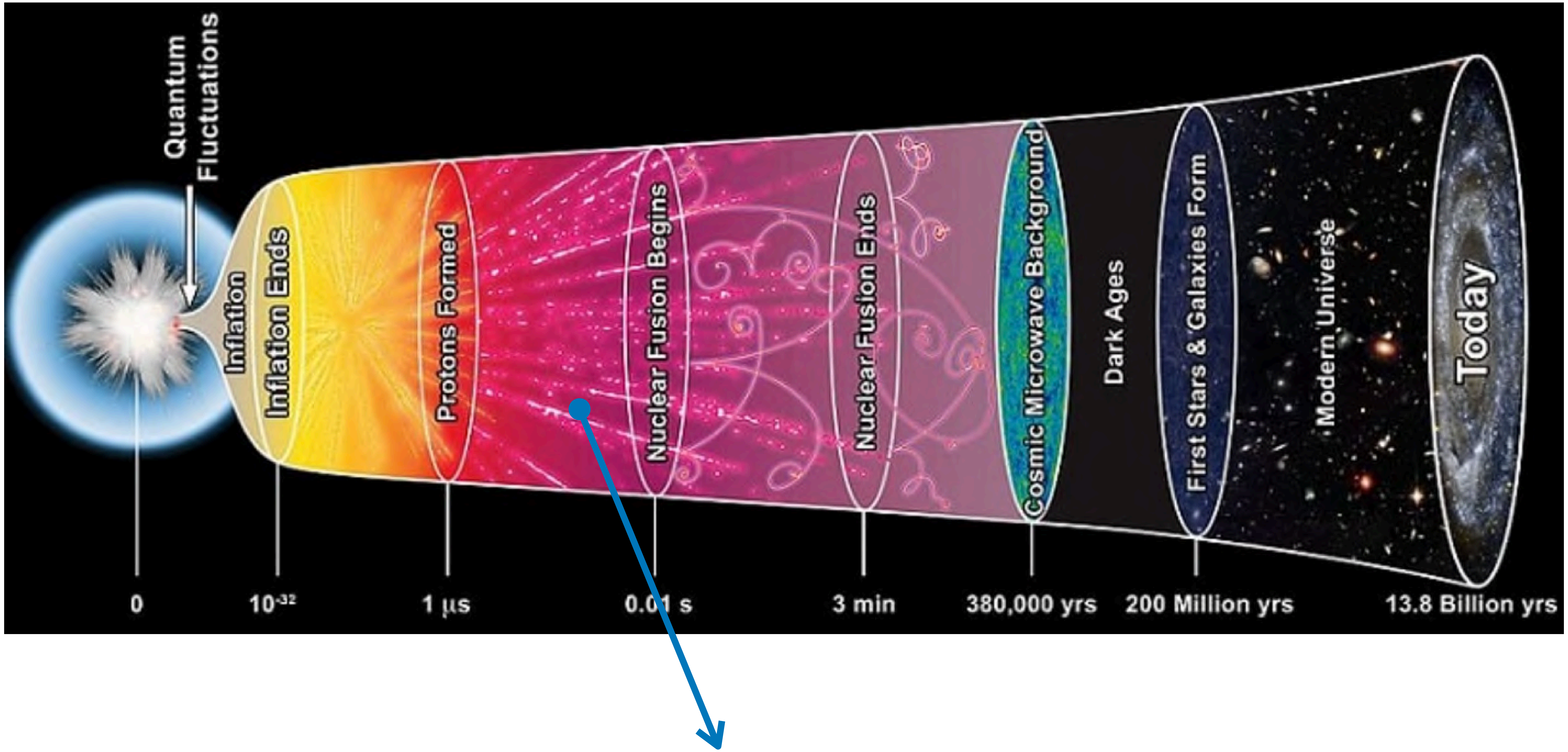

Radiation Dominated Era:

$$a(t) \propto t^{1/2}, \quad H = \frac{d\ln a}{dt} = \frac{1}{2t}$$

$$m_{pbh} \sim \frac{3H^2}{8\pi G} \times \frac{4\pi}{3} H^{-3} = \frac{H^{-1}}{2G} = \frac{t}{G} \sim 10^5 \left(\frac{t}{\text{sec}}\right) M_\odot$$

Hawking, 71'; Carr, Hawking, 74'

What is the nature of

Dark Matter?

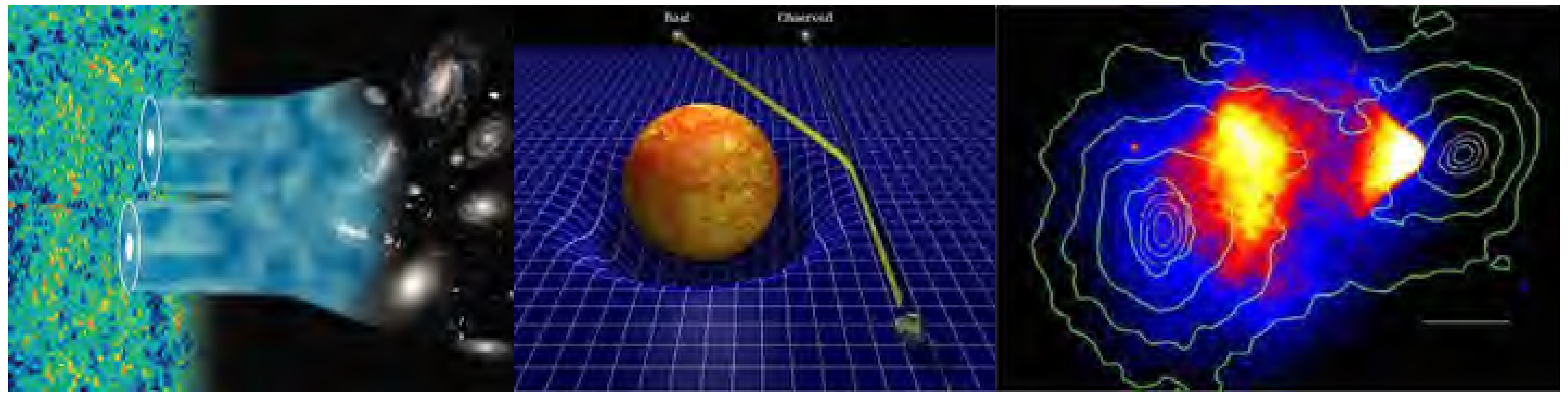

Planck 18 (CMB only): $\Omega_c h^2$ =0.1200±0.0012 (100σ)
Planck 18+BAO: $\Omega_c h^2$ =0.11933±0.00091 (131σ)

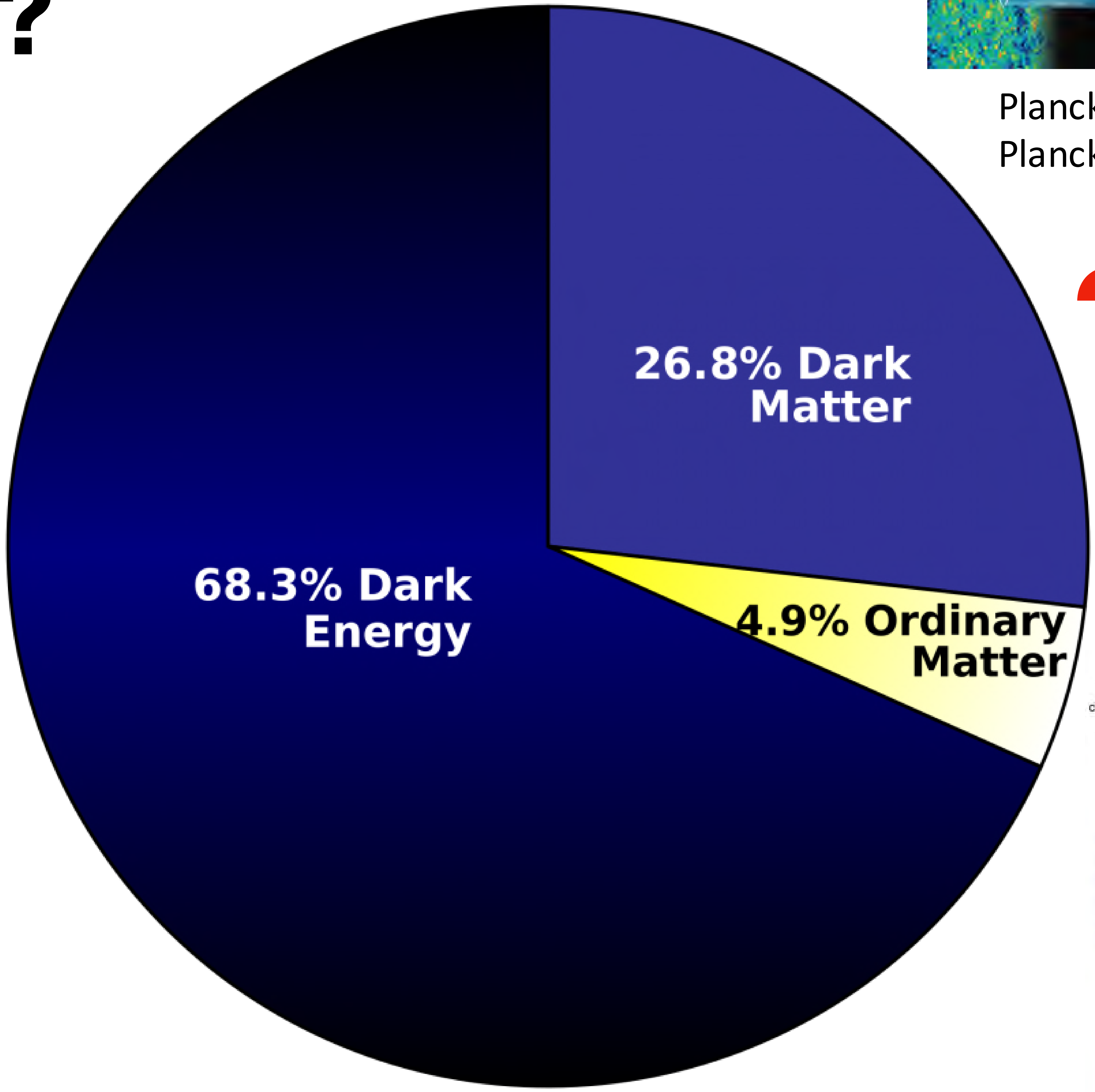

???

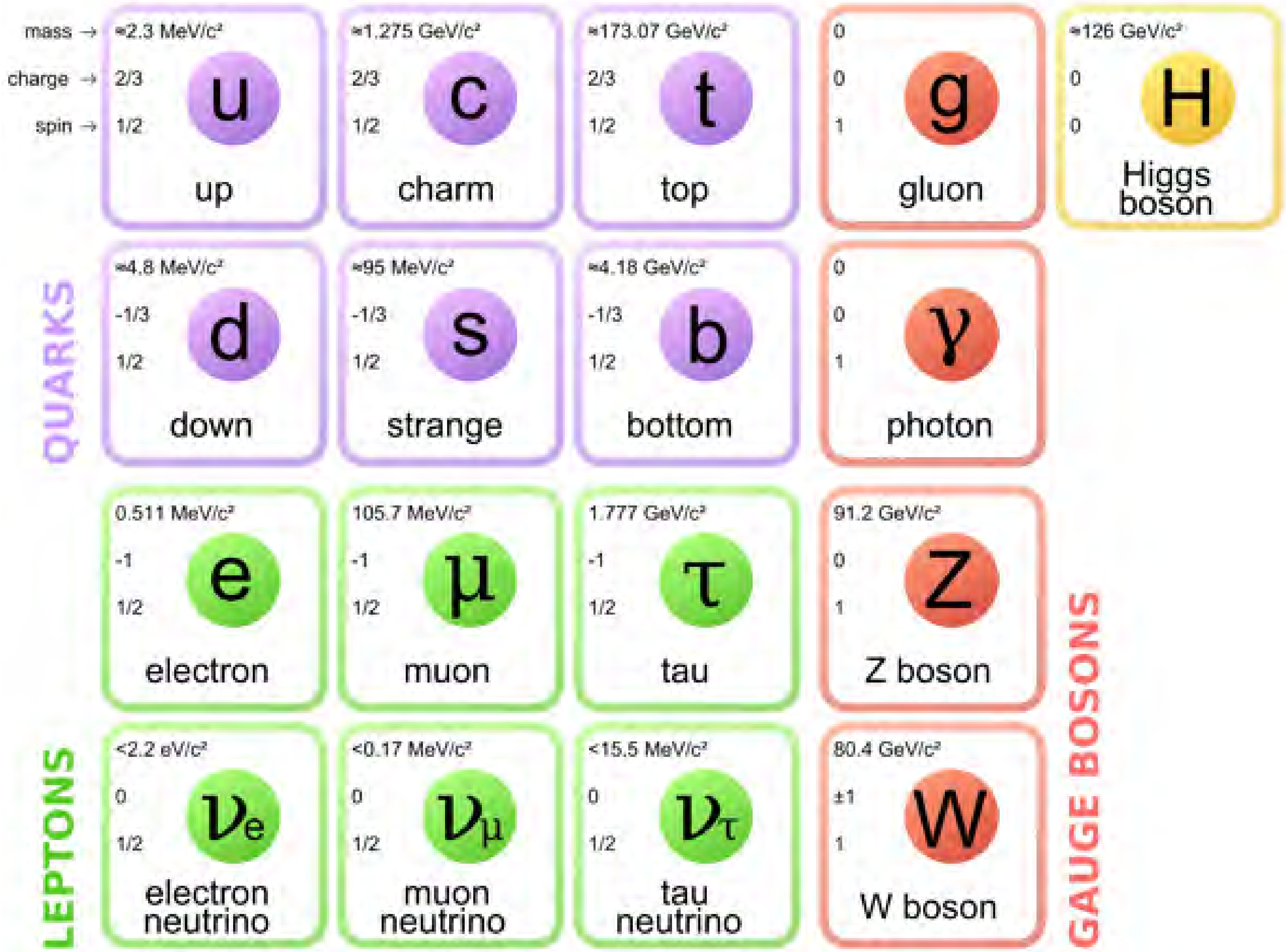

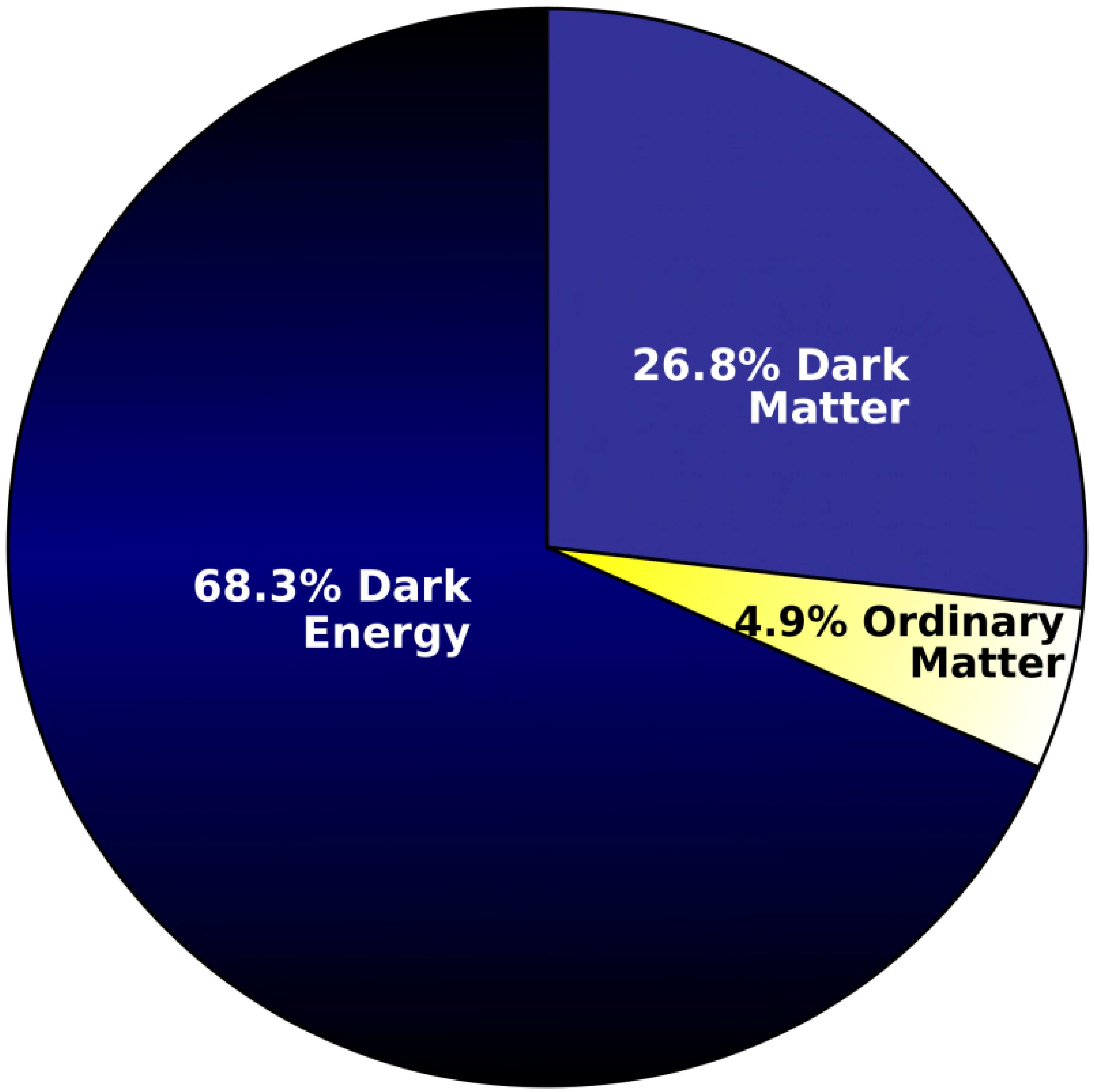

Primordial Black Hole (PBH)

$$f_{\rm pbh} = \frac{\Omega_{\rm pbh}}{\Omega_{CDM}}$$

- **PBH mass (function)**
- **Abundance of PBHs**

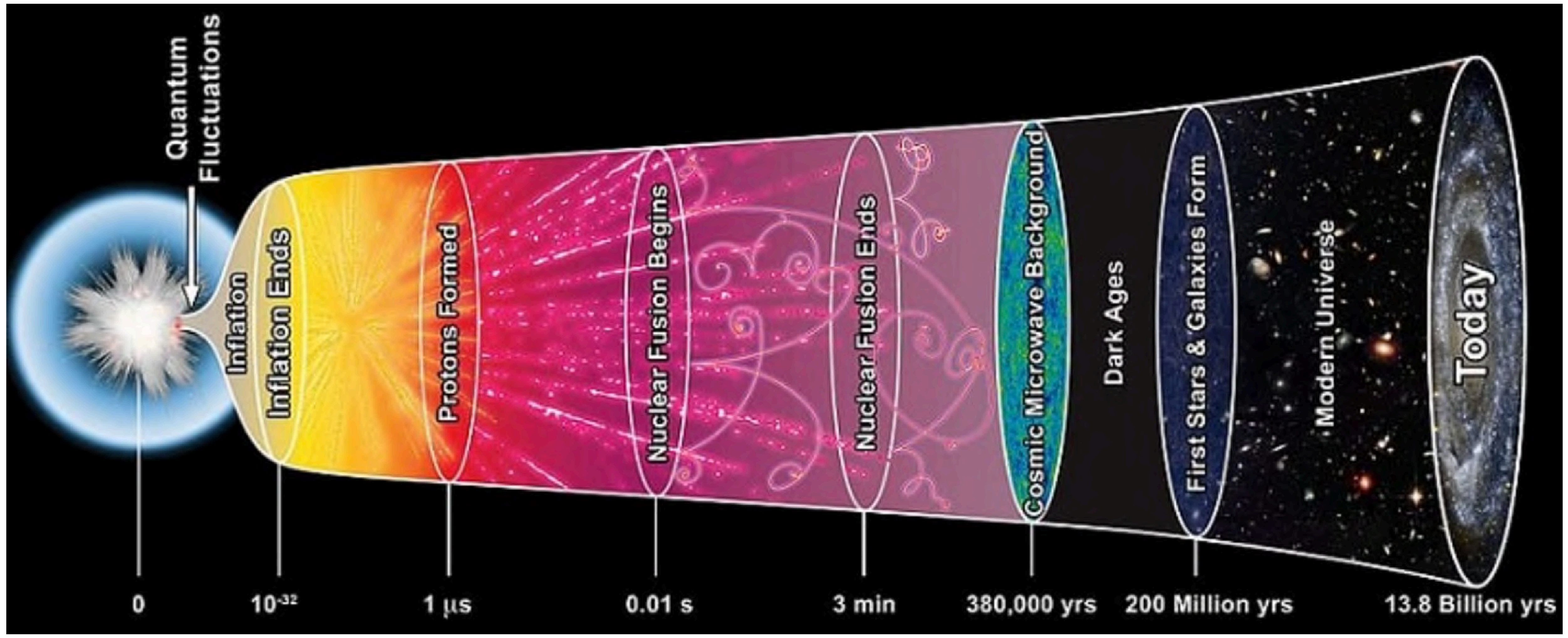

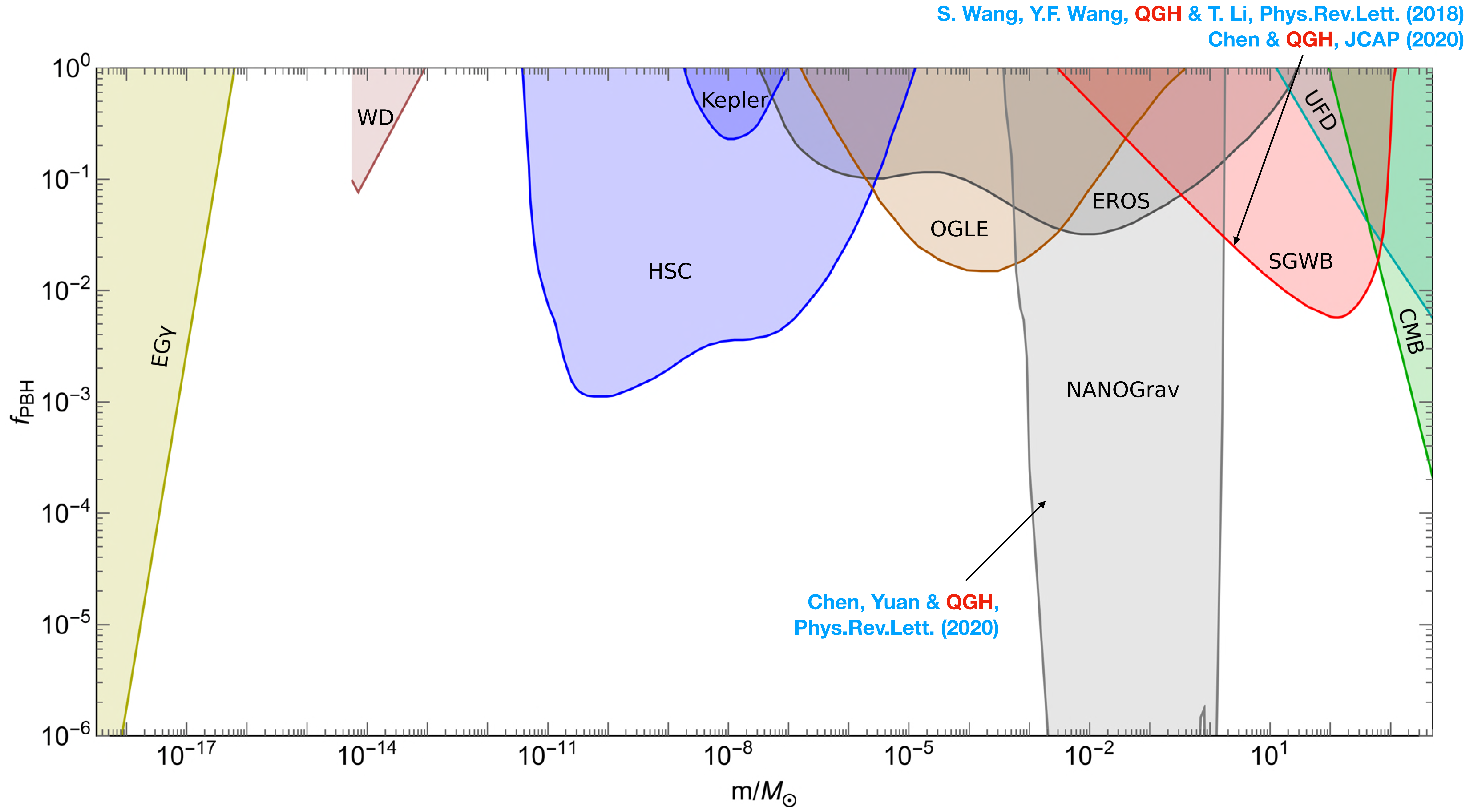

S. Wang, Y.F. Wang, QGH & T. Li, Phys.Rev.Lett. (2018)
Chen & QGH, JCAP (2020)
EGγ
WD
HSC
Kepler
OGLE
EROS
UFD
SGWB
CMB
NANOGrav
Chen, Yuan & QGH,
Phys.Rev.Lett. (2020)
f_{PBH}
$m/M_\odot$
10^0
10^{-1}
10^{-2}
10^{-3}
10^{-4}
10^{-5}
10^{-6}
10^{-17}
10^{-14}
10^{-11}
10^{-8}
10^{-5}
10^{-2}
10^{1}

Merger Rate & SGWB & SIGW

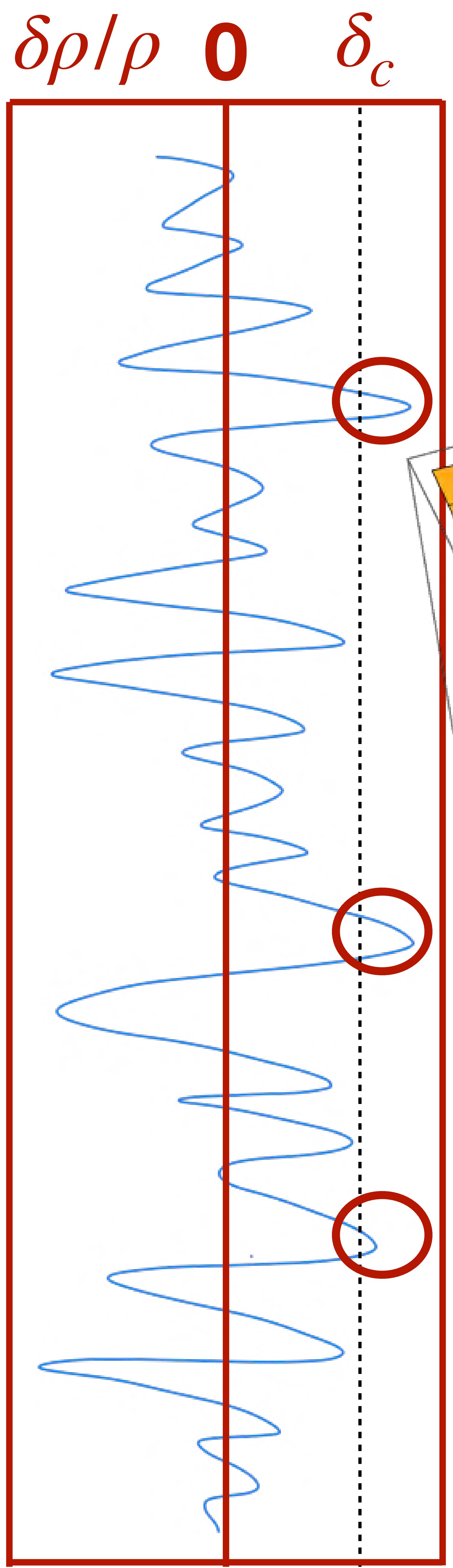

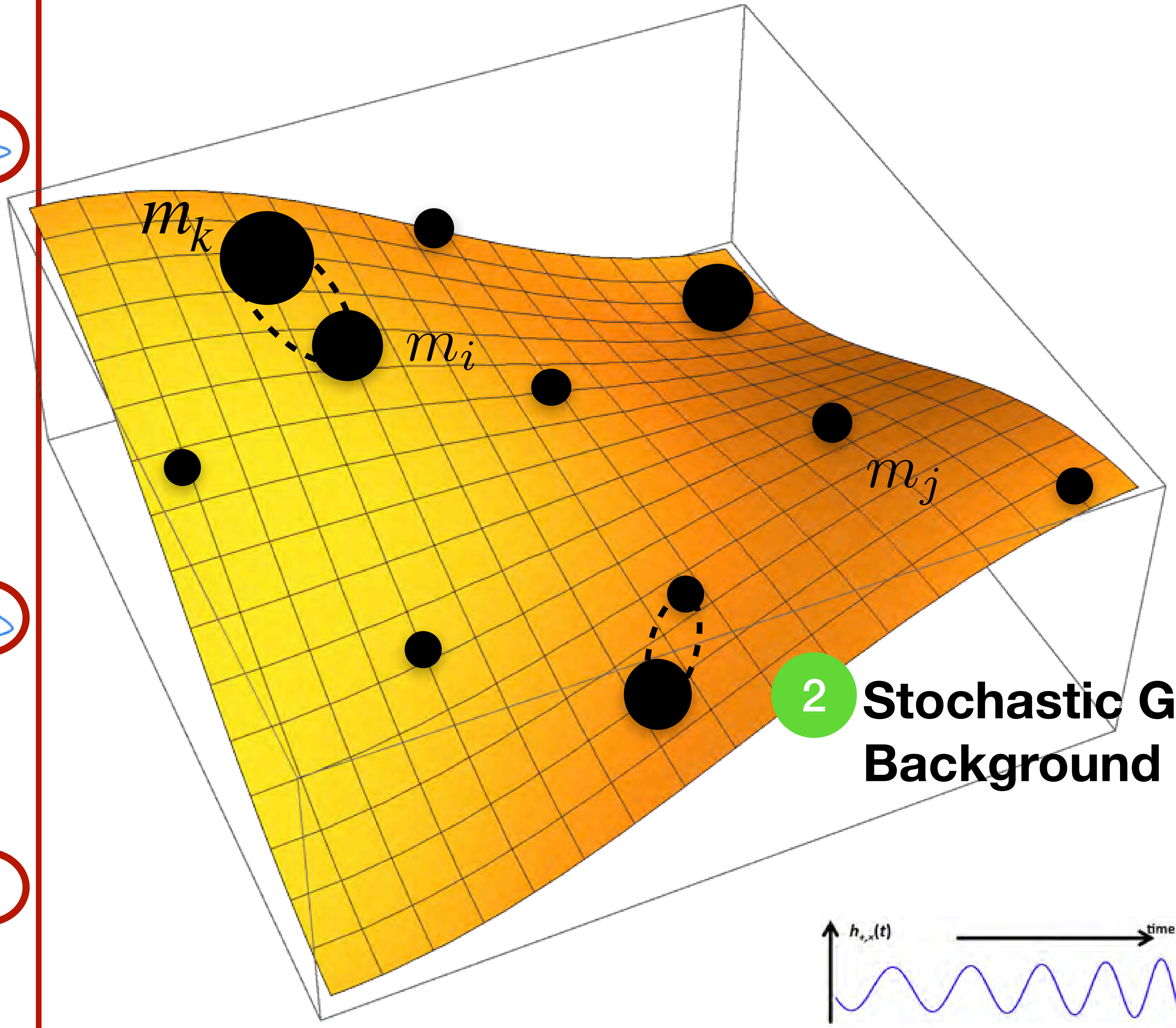

1 Merger rate distribution ($\text{Gpc}^{-3}\text{yr}^{-1}$)

$$R_{ij}(t) = \mathcal{R}_{ij}\Delta^2$$

$$\mathcal{R}_{ij} \simeq 3.9\cdot 10^6 \times \frac{\rho_m}{\rho_m^0}\left(\frac{t}{t_0}\right)^{-\frac{34}{37}} f^2(f^2+\sigma_{eq})^{-\frac{21}{74}} \times \min\left(\frac{P(m_i)}{m_i}, \frac{P(m_j)}{m_j}\right)\left(\frac{P(m_i)}{m_i}+\frac{P(m_j)}{m_j}\right) \times (m_i m_j)^{\frac{3}{37}}(m_i+m_j)^{\frac{36}{37}}$$

1. Decouple from the expansion of the background
2. Torques by all other PBHs and density perturbations provides an initial angular momentum
3. Coalescence due to GW radiations

Chen & QGH, ApJ (2018)

2 Stochastic Gravitational-Wave Background (SGWB)

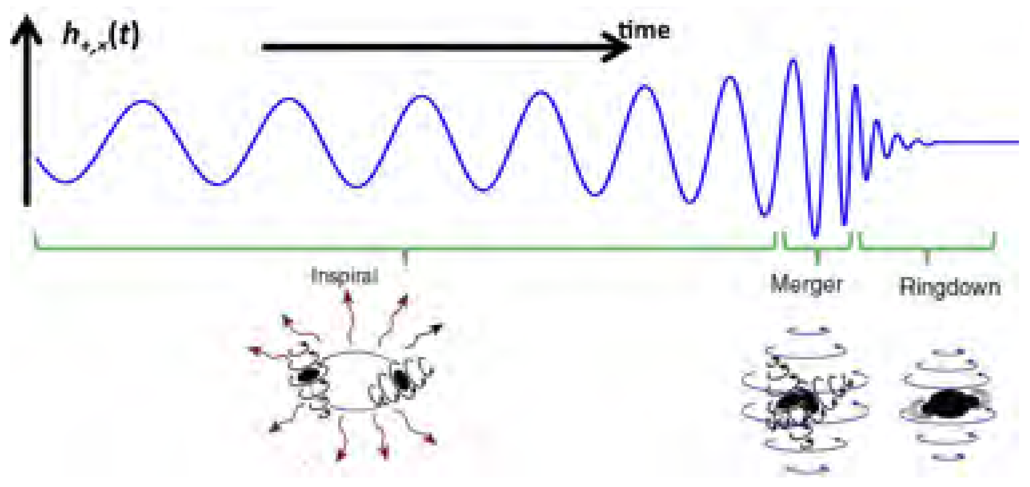

$$\Omega_{\rm GW}(\nu; M_{\rm PBH}, f) = \frac{\nu}{\rho_c H_0}\int_0^{z_{\rm sup}} \frac{R_{\rm PBH}(z; M_{\rm PBH}, f)}{(1+z)E(z)} \times \frac{dE_{\rm GW}}{d\nu_s}(\nu_s)dz,$$

Wang, Wang, QGH & Li, Phys.Rev.Lett. (2018)

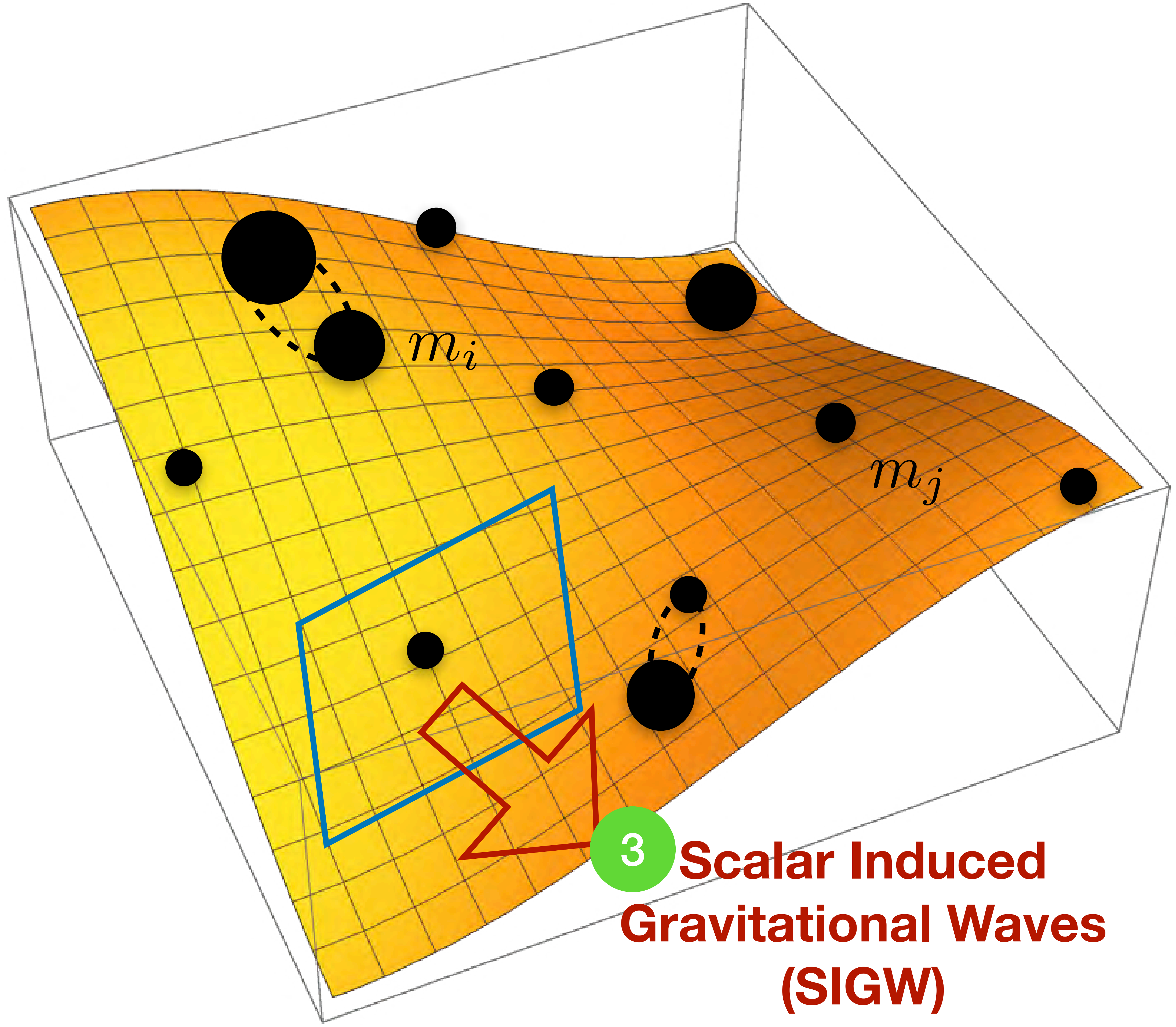

$$\mathrm{d}s^2 = a^2\left\{-(1+2\phi)\mathrm{d}\eta^2 + \left[(1-2\phi)\delta_{ij} + \frac{h_{ij}}{2}\right]\mathrm{d}x^i\mathrm{d}x^j\right\}$$

$$h''_{ij} + 2\mathcal{H}h'_{ij} - \nabla^2 h_{ij} = -4\mathcal{T}_{ij}^{\ell m}S_{\ell m}$$

$$S_{ij}^{(2)} = 4\phi\partial_i\partial_j\phi + 2\partial_i\phi\partial_j\phi - \frac{1}{\mathcal{H}^2}\partial_i(\mathcal{H}\phi+\phi')\partial_j(\mathcal{H}\phi+\phi')$$

Tomita, Prog. Theor. Phys. (1967)
Saito and Yokoyama, Phys.Rev.Lett. (2009)
Chen, Yuan & QGH, Phys.Rev.Lett. (2020)
……

$$\mathcal{R}_{ij} \simeq 3.9 \cdot 10^6 \times \frac{\rho_m}{\rho_m^0} \left(\frac{t}{t_0}\right)^{-\frac{34}{37}} f^2 (f^2 + \sigma_{eq})^{-\frac{21}{74}} \times \min\left(\frac{P(m_i)}{m_i}, \frac{P(m_j)}{m_j}\right) \left(\frac{P(m_i)}{m_i} + \frac{P(m_j)}{m_j}\right) \times (m_i m_j)^{\frac{3}{37}} (m_i + m_j)^{\frac{36}{37}}$$

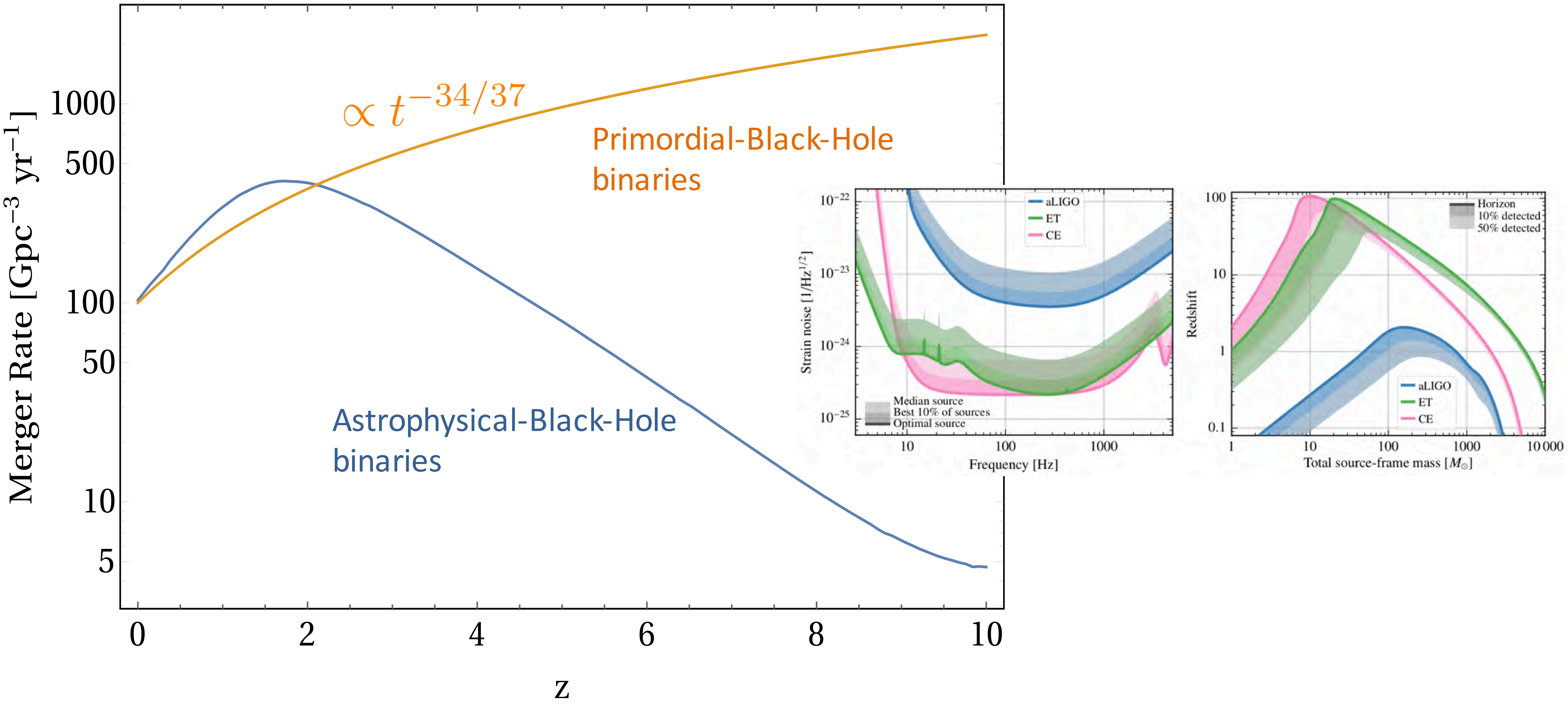

Chen & QGH, ApJ (2018) & JCAP (2020)

Scalar induced GWs and Pulsar Timing Array

For $m_{pbh} \sim 10 M_{\odot}$,

$$\lambda_{GW} \sim \frac{T_{QCD}}{T_0} \times 10 \text{ km} \sim 10^{13} \text{ km}$$

$$\sim 10^{8} \text{ sec} \sim 10 \text{ year}$$

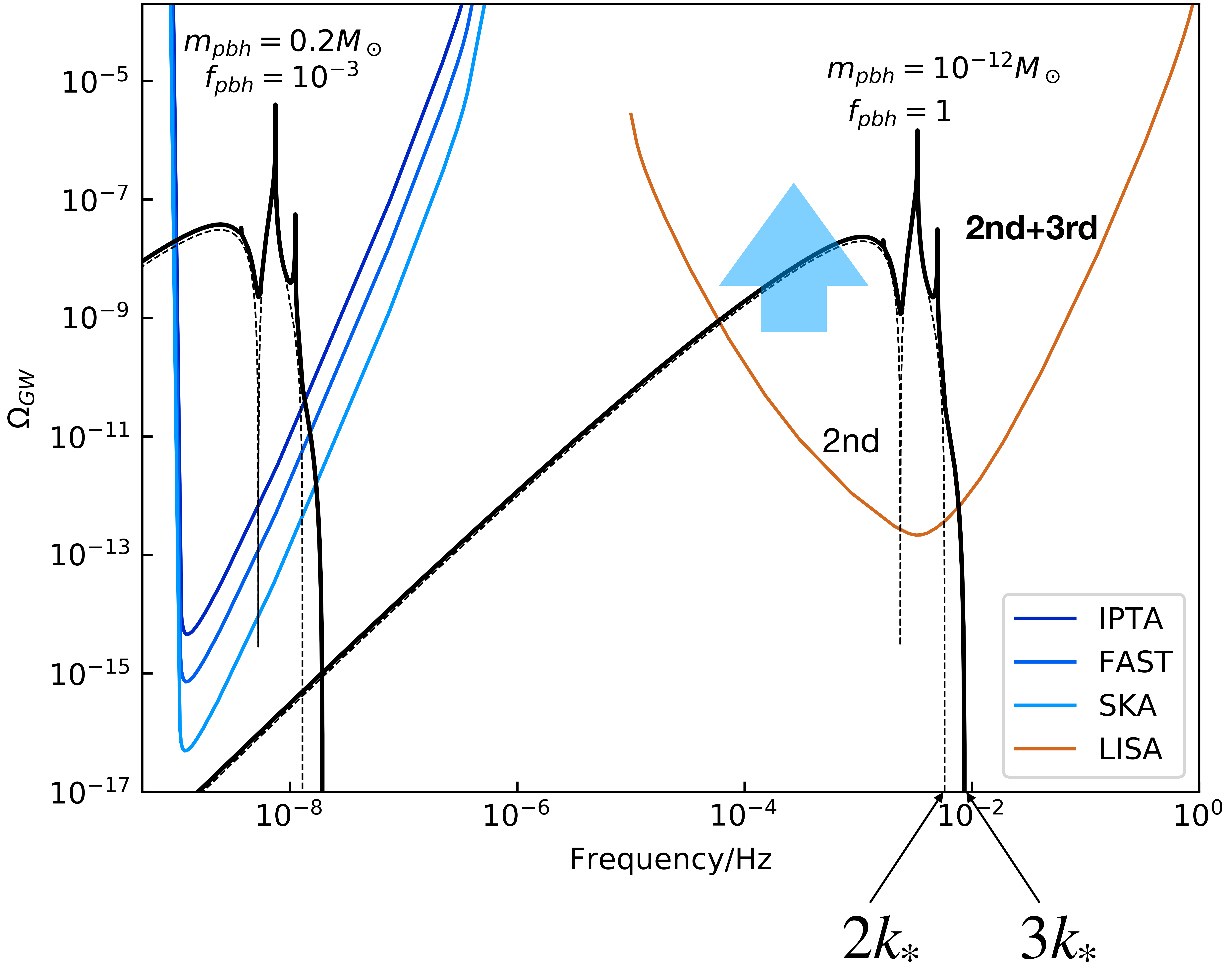

Yuan, Chen & QGH, Phys.Rev.D (rapid) (2019)

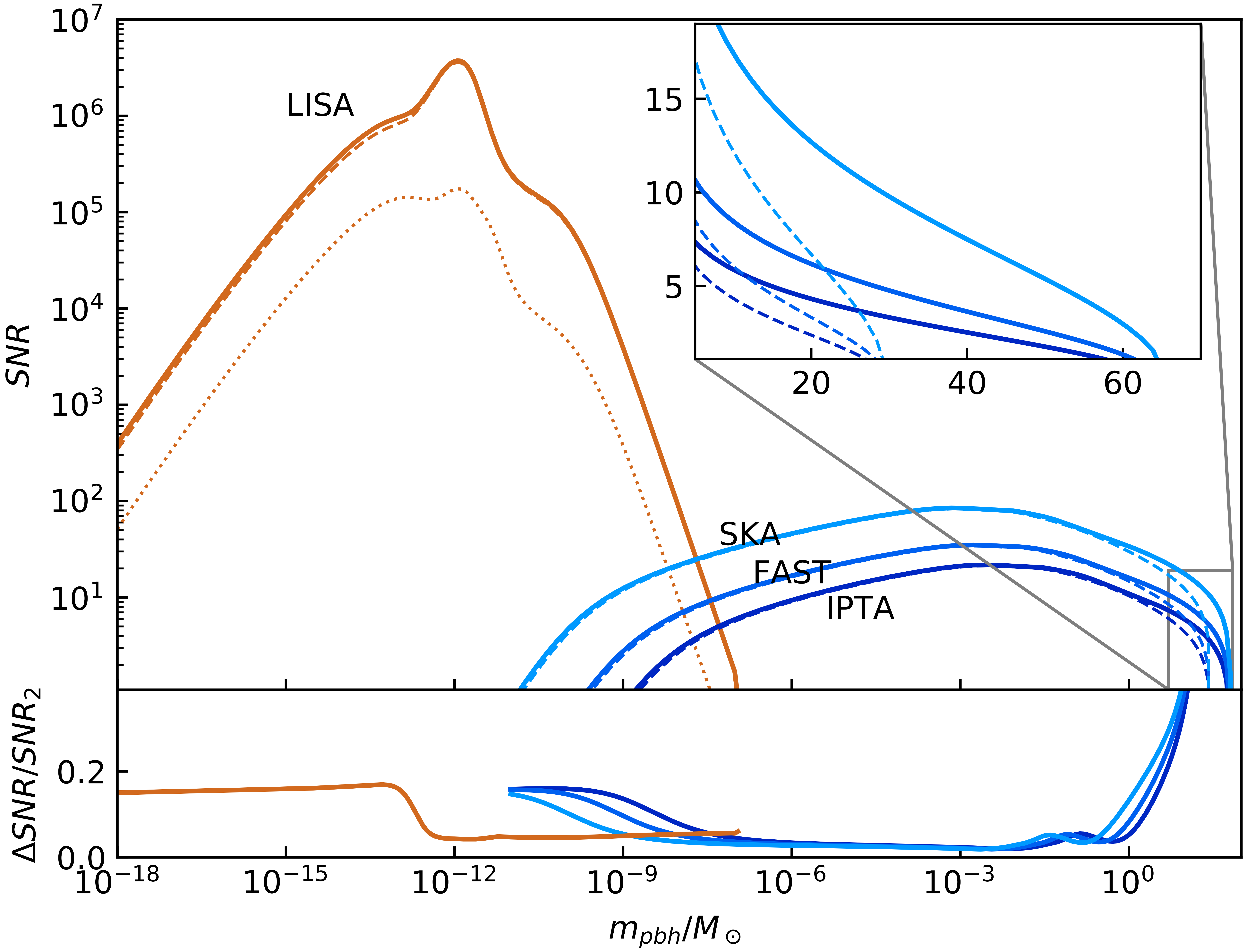

Yuan, Chen & QGH, Phys.Rev.D (rapid) (2019)

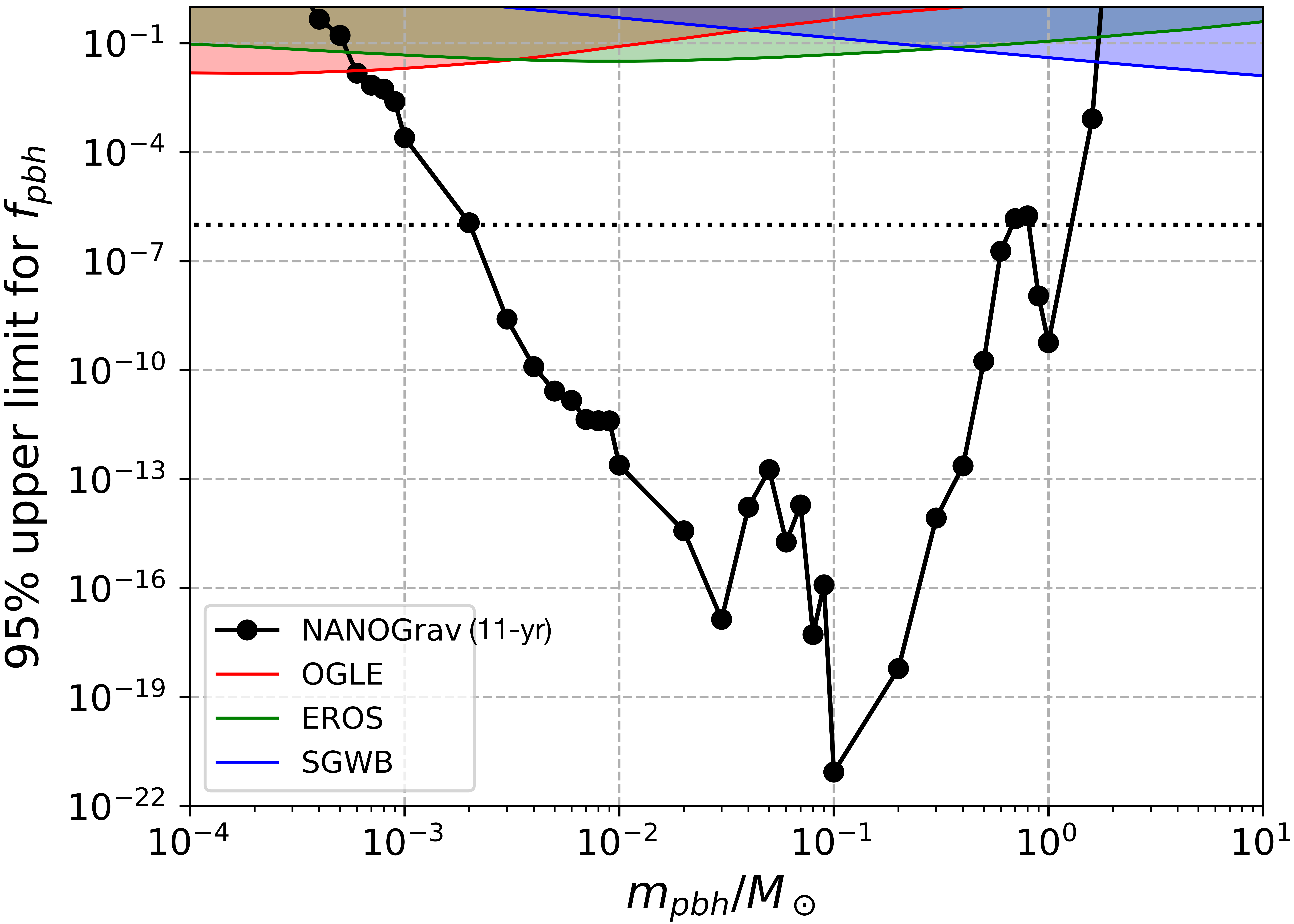

Chen, Yuan & QGH, Phys.Rev.Lett. (2020)

The superposition of GWs from various sources in the Universe forms a stochastic GW background.

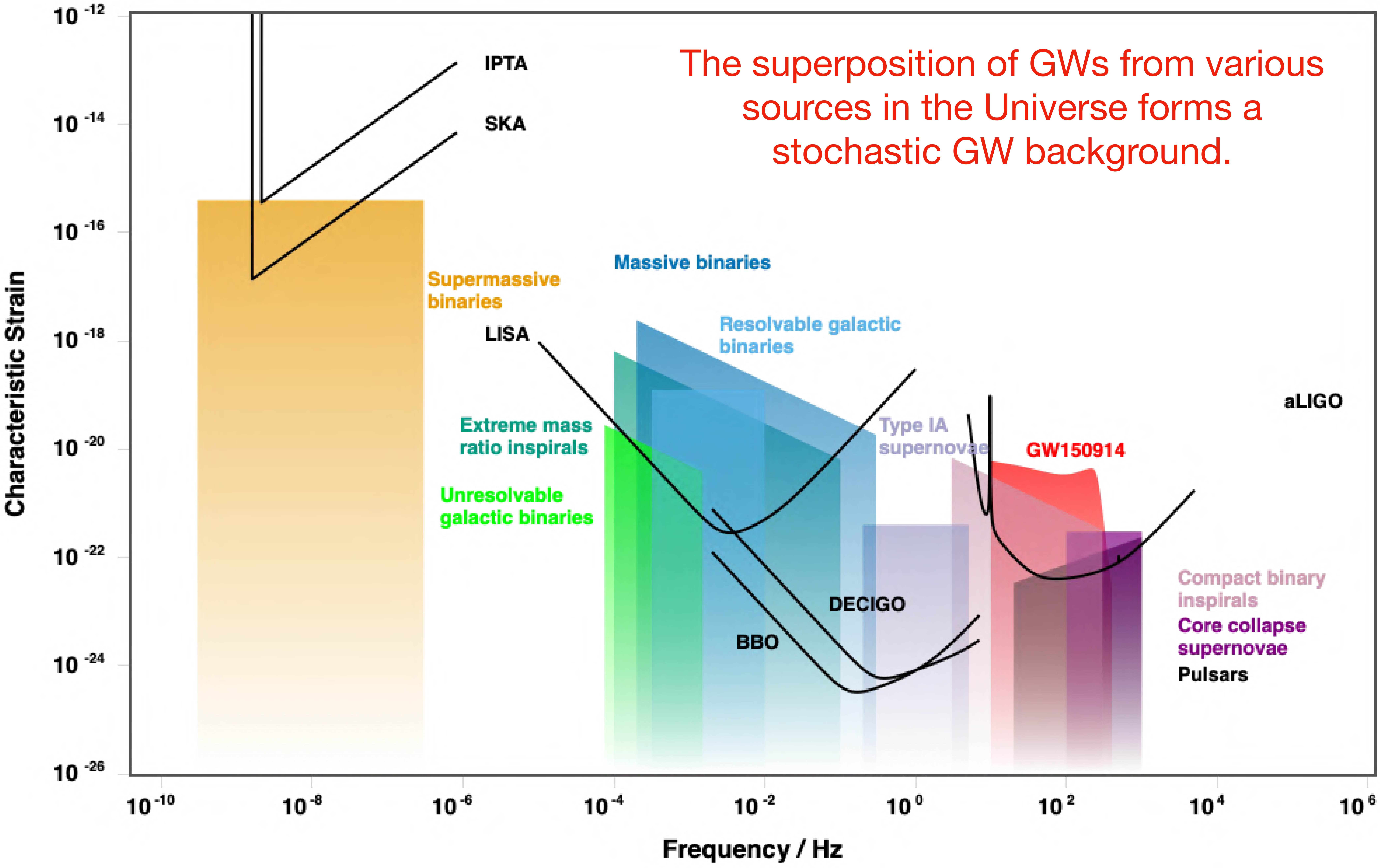

$$\Omega_{GW}(f) = \frac{1}{\rho_c}\frac{d\log\rho_{GW}}{d\log f} = \frac{\pi^2}{3H_0^2} f^3 S_h(f) \propto f^{n_{GW}}$$

slope

GW spectral energy density

spectral density

$n_{GW} = 2/3$

Compact Binary Coalescences

$n_{GW} = n_t + \alpha_t \ln(f/f_{CMB})/2$

Primordial Gravitational Waves

$n_t \simeq 0,\ \alpha_t \simeq 0$

$n_{GW} = 0$

Scale-invariant Energy

$n_{GW} = 3\ or\ 2 - 2/\ln(f_c/f)$

Scalar induced GWs
inevitably accompanying the formation of PBHs

Yuan, Chen & QGH, Phys.Rev.D (2020)

NANOGrav 12.5-year data

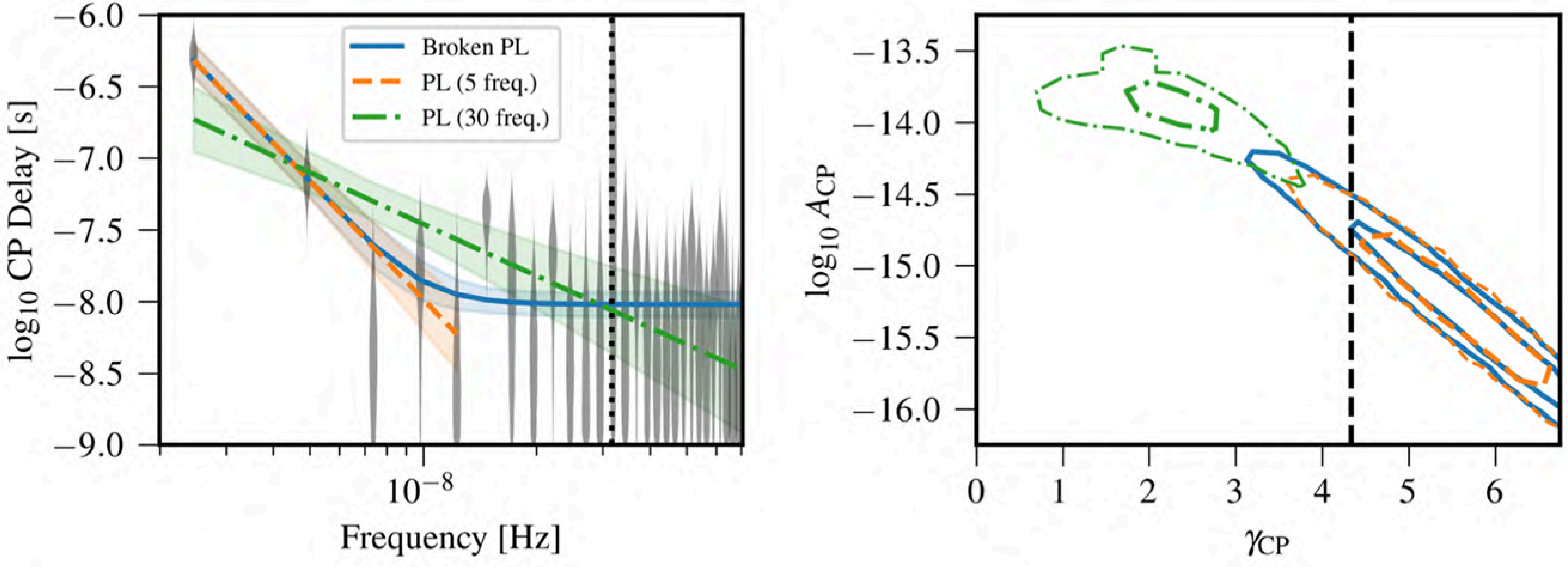

Figure 1. Posteriors for a common-spectrum process in NG12, as recovered with four models: free-spectrum (gray violin plots in left panel), broken power law (solid blue lines and contours), 5-frequency power law (dashed orange lines and contours), and 30-frequency power law (dot-dashed green lines and contours). In the left panel, the violin plots show marginalized posteriors

Our analysis finds strong evidence of a stochastic process, modeled as a power-law, with common amplitude and spectral slope across pulsars.

However, we find **NO** statistically significant evidence that this process has quadrupolar spatial correlations, which we would consider necessary to claim a GWB detection consistent with GR.

NANOGrav Collaboration, ApJL 905 (2020) 2

Gravitational–Wave Polarization

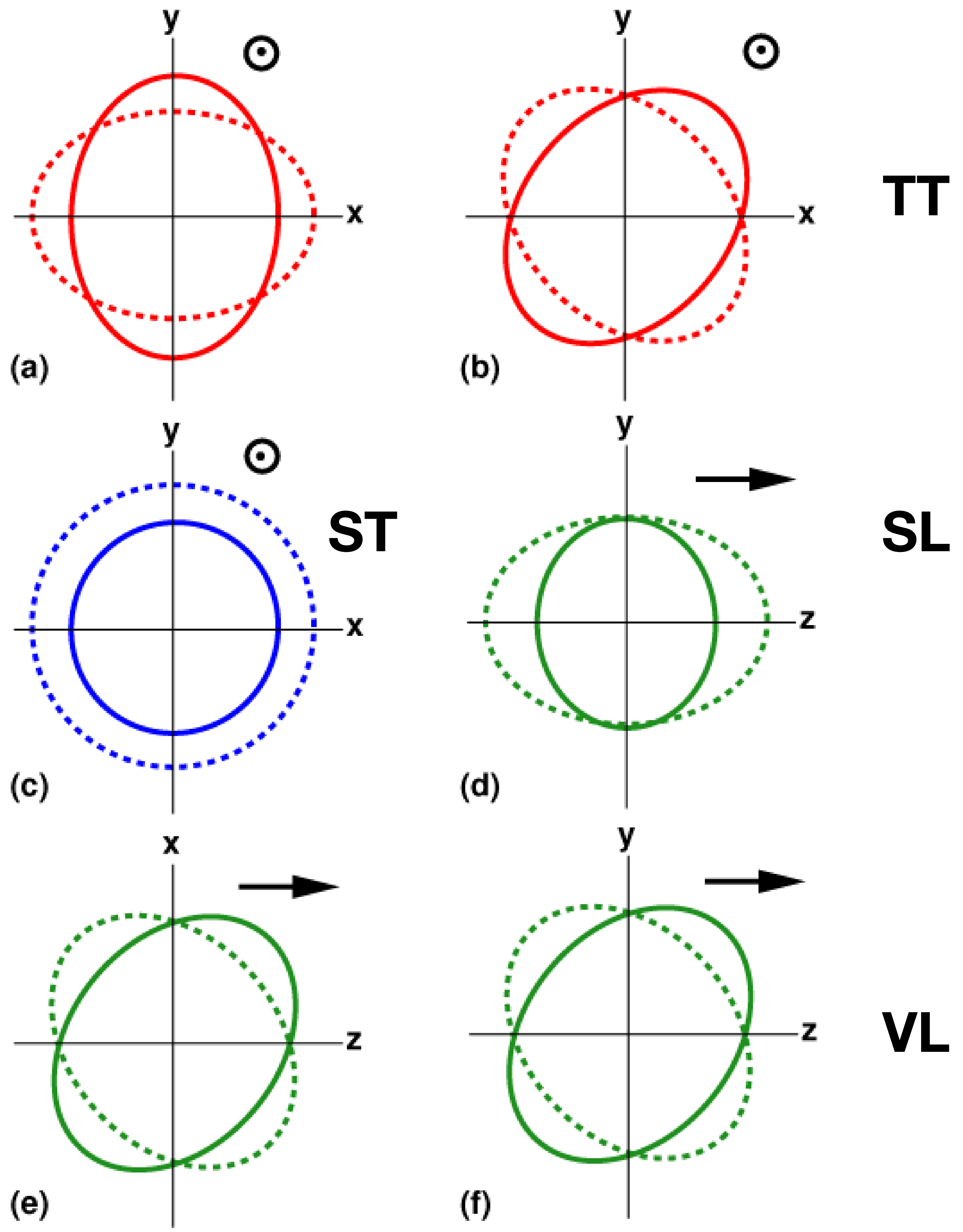

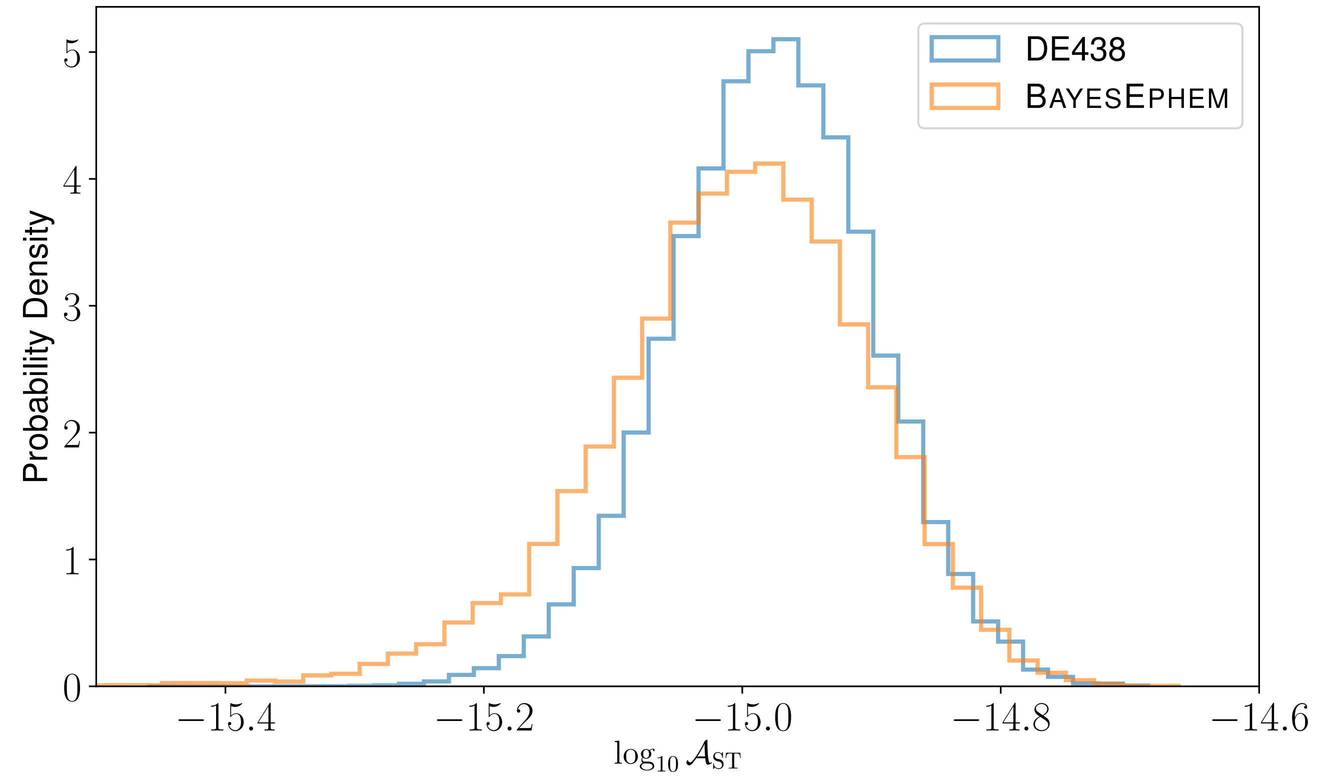

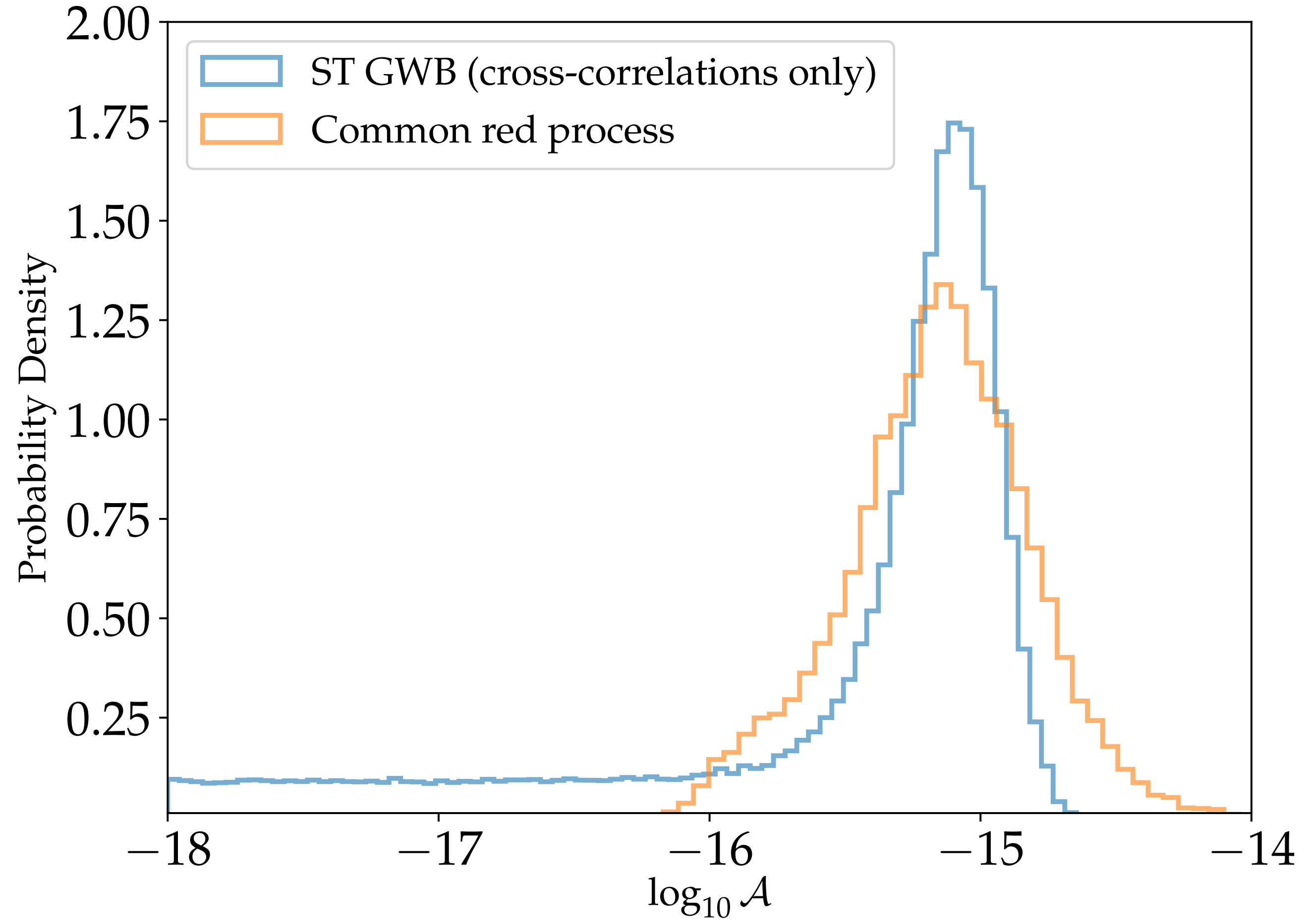

$$\frac{h^{ST}(f)}{h^{TT}(f)} \sim f^{-1/3}, \quad \textbf{or}, \quad \frac{\Omega^{ST}_{GW}(f)}{\Omega^{TT}_{GW}(f)} \sim f^{-2/3}$$

ephemeris	TT	ST	VL	SL
DE438	4.96(9)	107(7)	1.94(3)	0.373(5)
BayesEphem	2.35(3)	18.4(7)	1.31(2)	0.555(7)

Strong Bayesian Evidence

TABLE II. The Bayes factors for various models compared to the UCP model. The digit in the parentheses gives the uncertainty on the last quoted digit.

$$A_{ST} = 1.06^{+0.35}_{-0.28} \times 10^{-15}, \textbf{ or, } \Omega^{ST}_{GW} = 1.54^{+1.21}_{-0.71} \times 10^{-9}$$

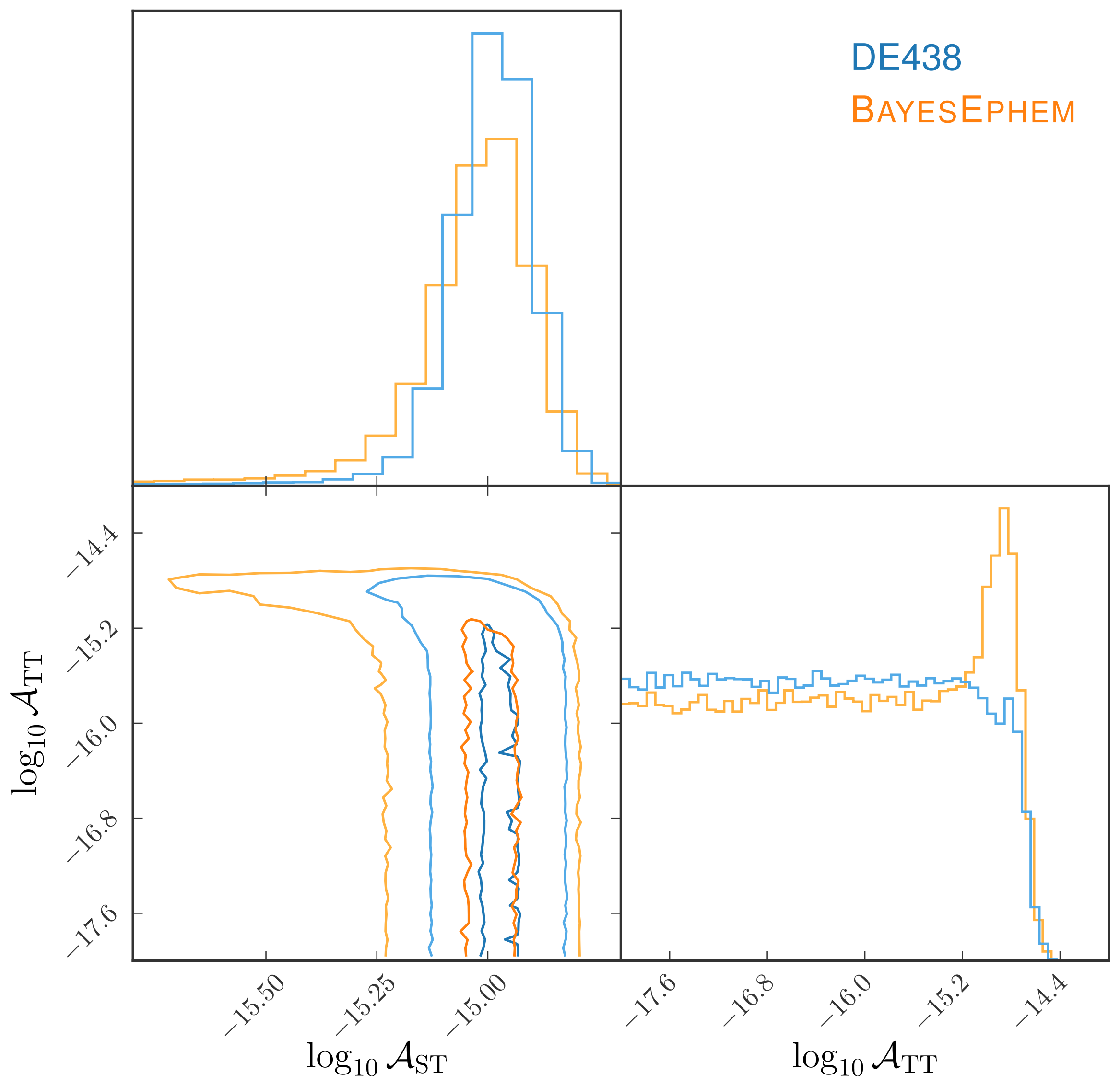

NANOGrav 11 yr:

$$A_{TT} < 1.94 \times 10^{-15}$$

NANOGrav 12.5 yr (after subtracting ST mode)

$$A_{TT} < 1.48 \times 10^{-15}$$

Chen, Yuan & QGH, arXiv:2101.06869

Parkes Pulsar Timing Array Second Data Release

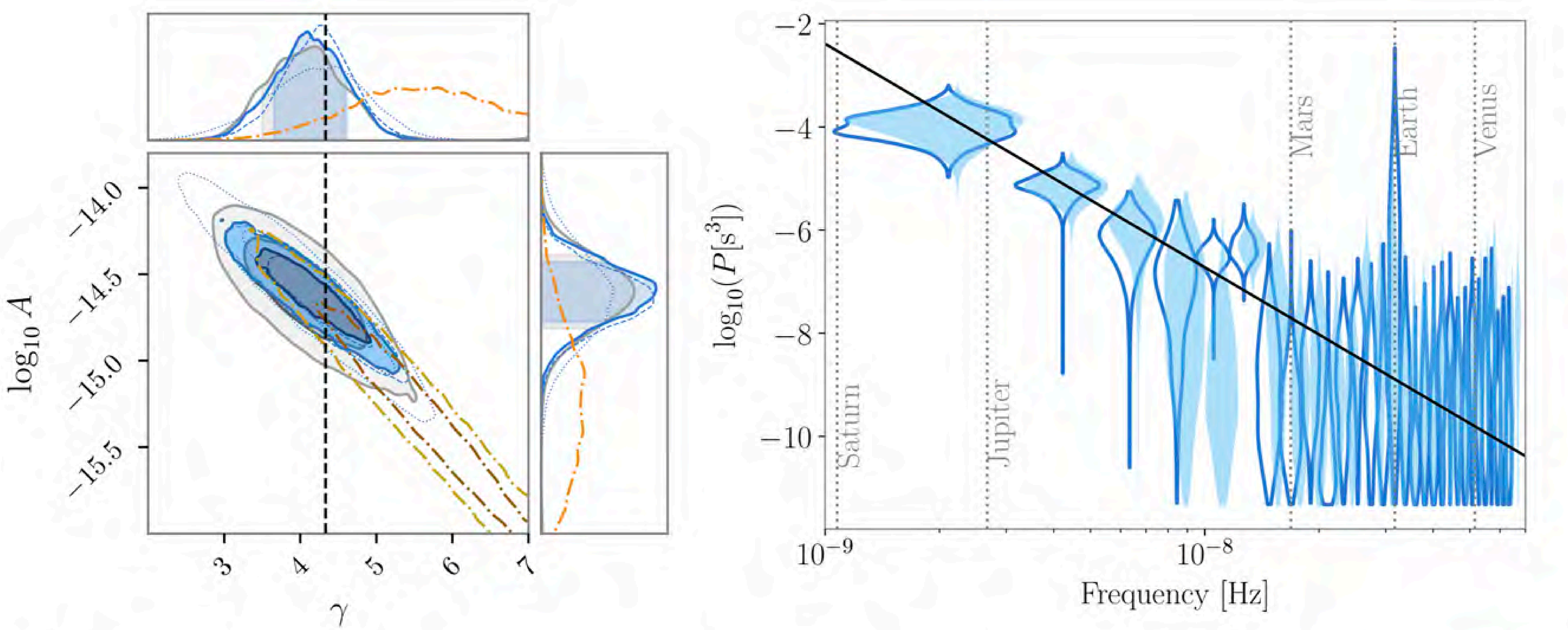

Figure 1. Left: Measurements of common power-law red-noise parameters and the demonstration of their robustness to assumptions about pulsar-intrinsic noise and the number of fluctuation frequencies n_c. The dashed vertical line indicates $\gamma = 13/3$. The solid lines represent the measurement based on $n_c = 30$. Dashed and dotted lines represent $n_c = 20$ and $n_c = 5$. The dash-dotted lines correspond to the measurement from Arzoumanian et al. (2020). Contours and shaded regions are 1-σ and 2-σ credible levels. Grey lines and regions are based on the assumption of achromatic timing noise in every pulsar, whereas blue ones are based on the assumption of timing noise only in pulsars where it was reported in Goncharov et al. (2020b). Right: Common red-noise parameter estimation with the free-spectral model. Lines represent the full PPTA data, whereas filled regions represent PPTA DR2 without PSR J0437−4715. The black line is the inferred spectrum assuming a power-law model with $\gamma = 13/3$. Vertical dotted lines represent inverse orbital periods of solar system planets.

Goncharov et al., arXiv:2107.12112

Model	TT	ST	VL	SL
BF	2.15(4)	0.183(3)	1.06(2)	0.362(6)

Table 3. Bayes factors of the TT, ST, VL, and SL models compared to the UCP model. The digit in the parentheses gives the uncertainty on the last quoted digit.

	Ω_{GW}^{TT}	Ω_{GW}^{ST}	Ω_{GW}^{VL}	Ω_{GW}^{SL}
TT/ST/VL/SL	1.4×10^{-8}	4.5×10^{-9}	1.7×10^{-10}	2.4×10^{-12}
TT+ST+VL+SL	1.2×10^{-8}	1.4×10^{-9}	1.2×10^{-10}	1.0×10^{-12}

Table 4. The 95% upper limit of energy density parameter per logarithm frequency Ω_{GW} at frequency of 1/year from the process with either the TT, ST, VL or SL correlations (the TT/ST/VL/SL model) and the process with all the correlations (the TT+ST+VL+SL model).

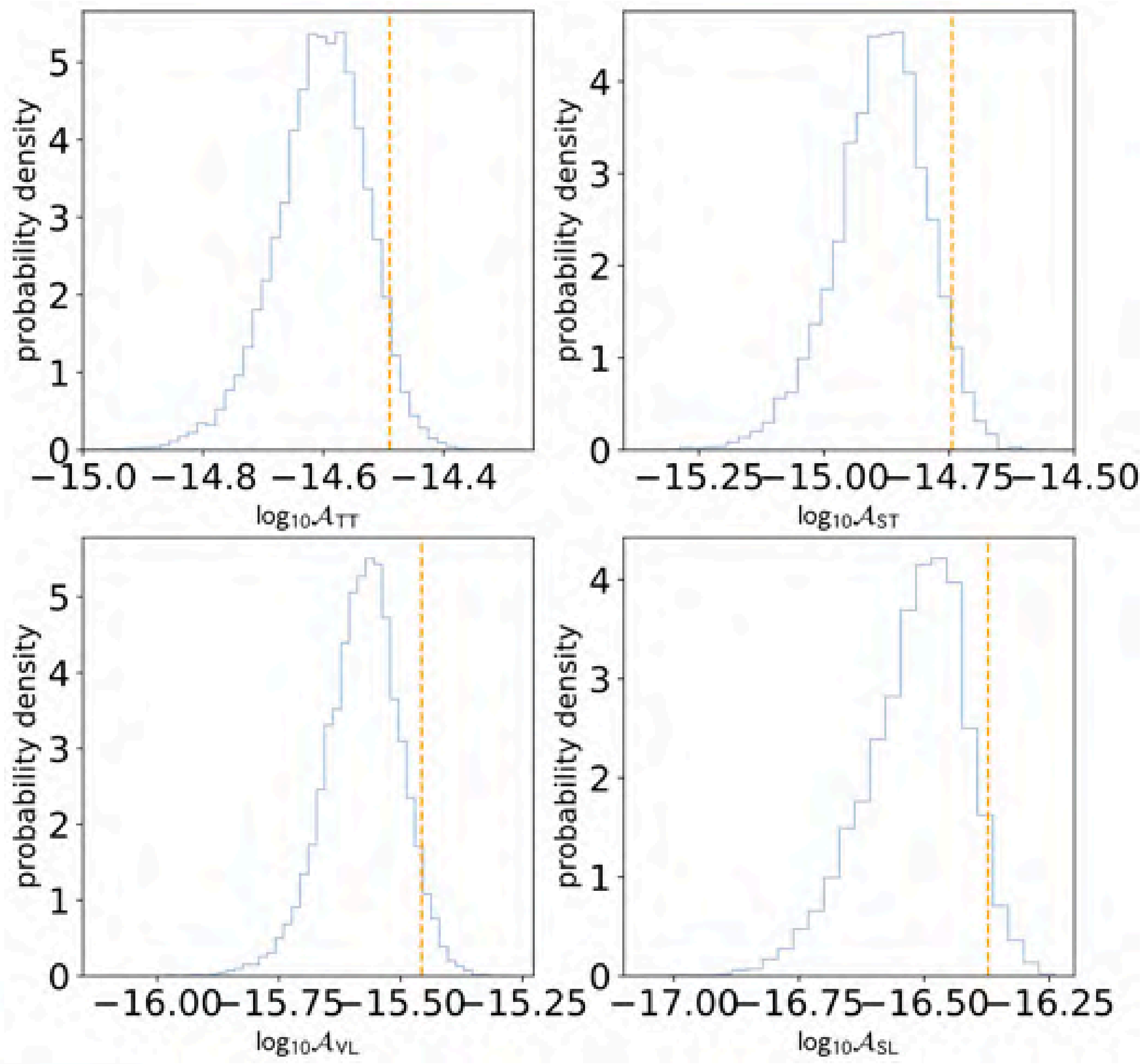

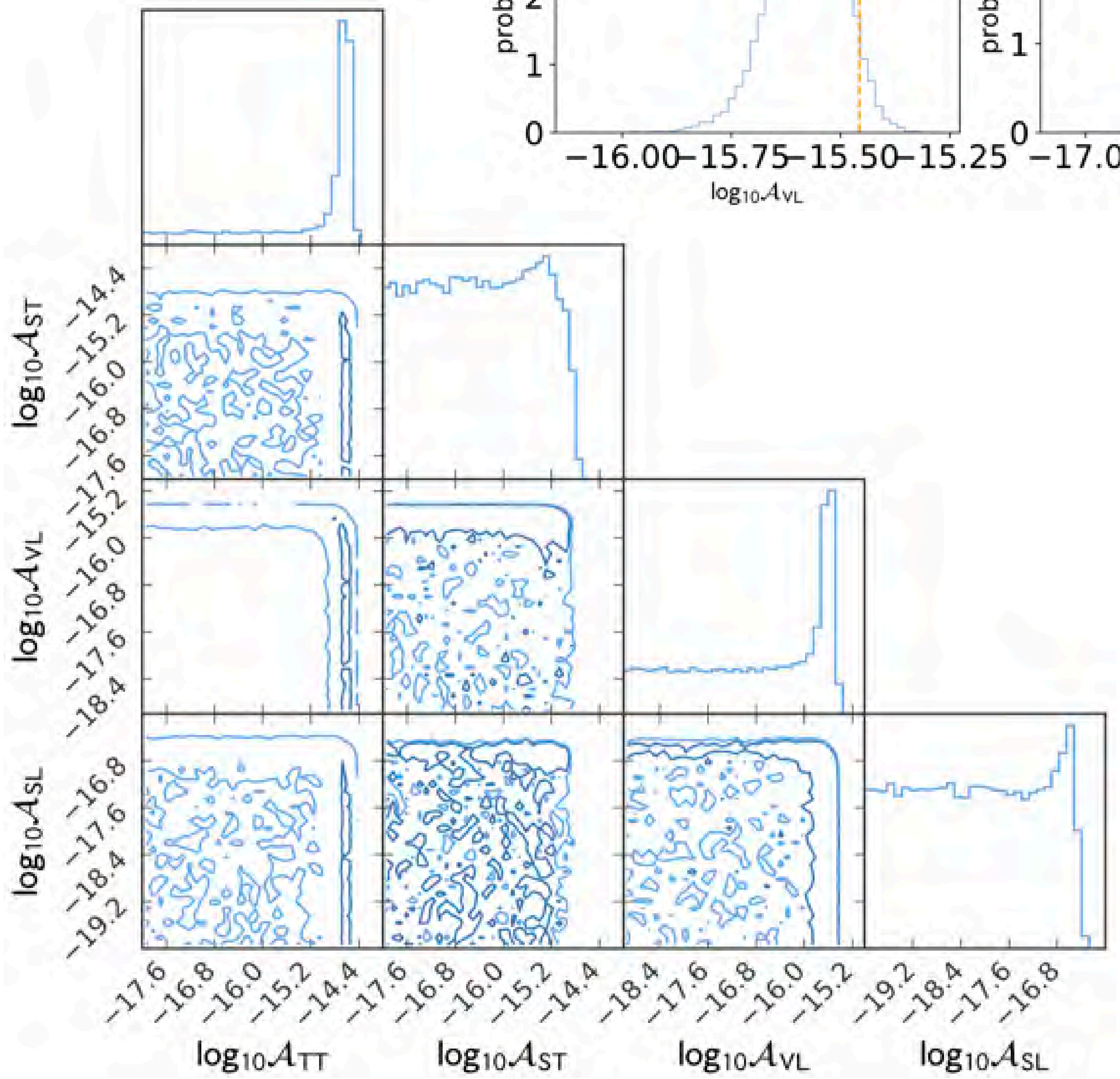

We did not find any evidence for the tensor transverse (TT), scalar transverse (ST), vector longitudinal (VL), and scalar longitudinal (SL) correlations in PPTA second data release (DR2).

The upper limits on ST mode from PPTA DR2 is consistent with what we found in NANOGrav 12.5-yr data.

Wu, Chen & QGH, arXiv:2108.10518

International Pulsar Timing Array Second Data Release

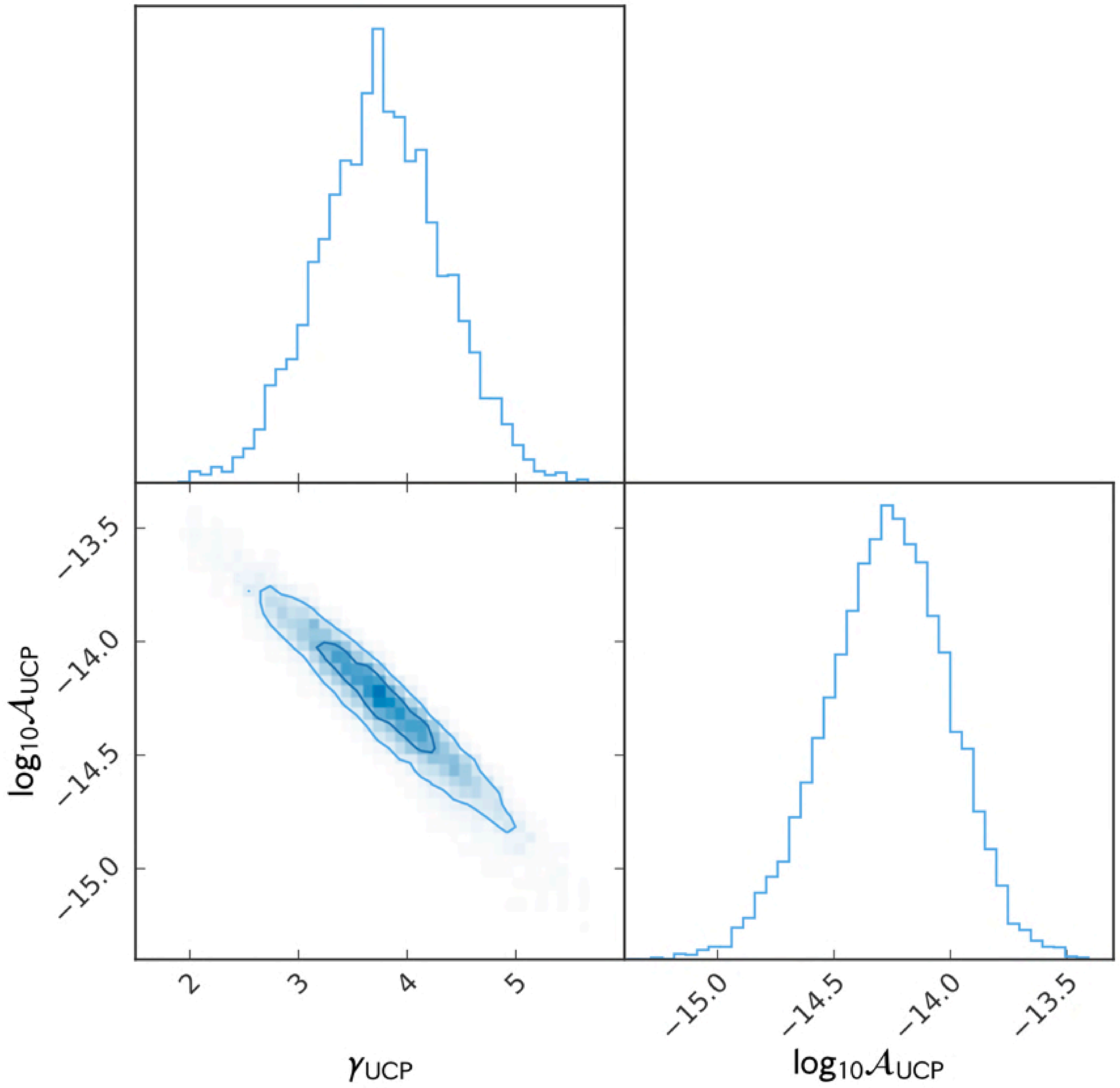

Chen, Wu & QGH, arXiv:2109.00296

$$\Omega_{GW}^{ST} = 2.31^{+2.19}_{-1.30} \times 10^{-9}$$ **(ST only)**

$$\Omega_{GW}^{ST} = 1.71^{+2.48}_{-1.70} \times 10^{-9}$$ **(ST+TT)**

consistent with NANOGrav 12.5-yr

$$\Omega_{GW}^{TT} < 2.16 \times 10^{-8}$$ **(TT only)**

$$\Omega_{GW}^{TT} < 1.48 \times 10^{-8}$$ **(ST+TT)**

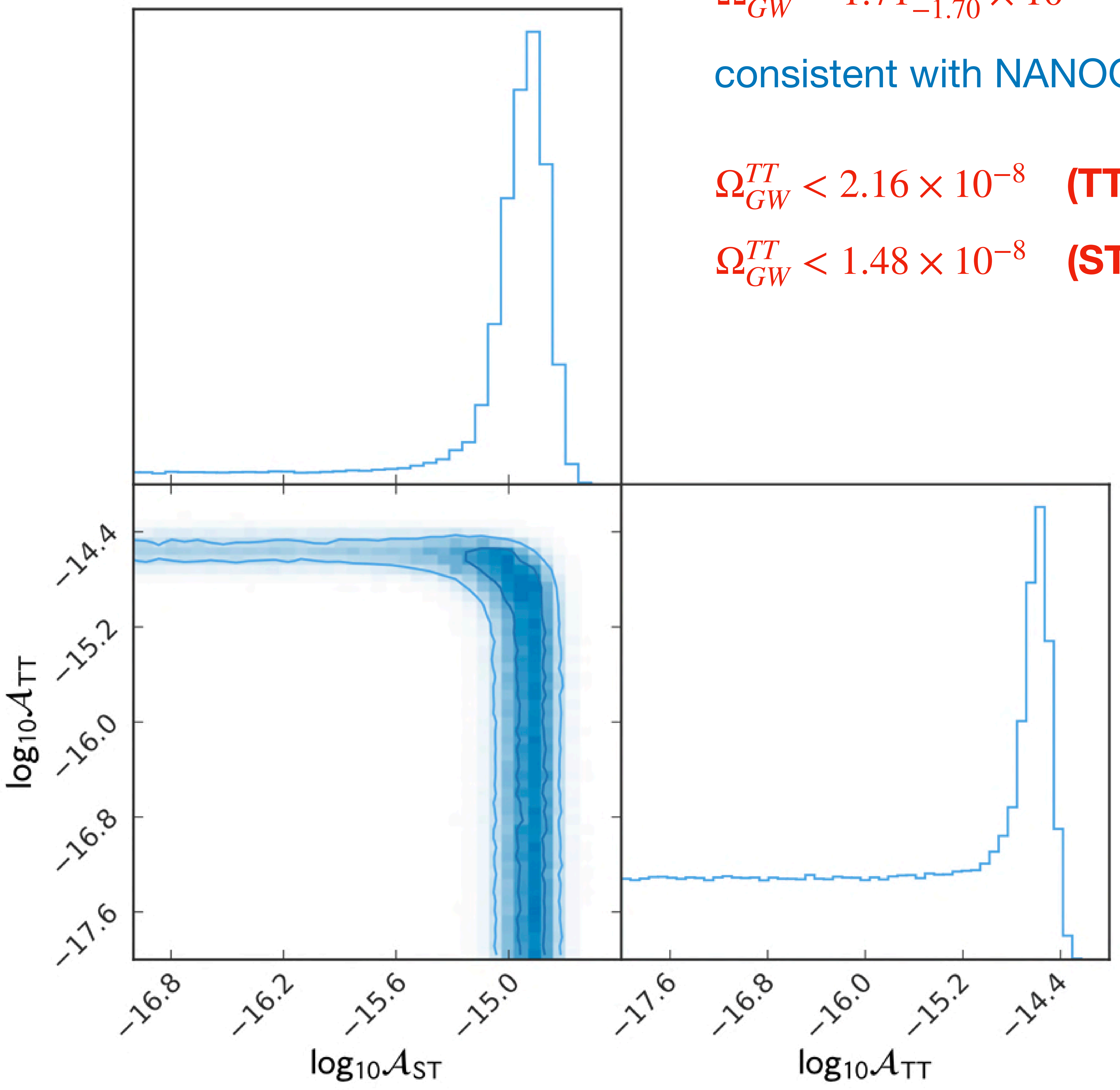

$\mathcal{BF}$	$\ln \mathcal{BF}$	Strength of evidence
< 1	< 0	Negative
$1 - 3$	$0 - 1$	Not worth more than a bare mention
$3 - 20$	$1 - 3$	Positive
$20 - 150$	$3 - 5$	Strong
> 150	> 5	Very strong

UCP vs. NO	TT vs. UCP	ST vs. UCP	ST+TT vs. UCP
10.5(9)	2.53(3)	3.39(4)	3.63(4)

Table 3. The $\ln \mathcal{BF}$ between pairs of models. The digit in the parentheses represents the uncertainty on the last quoted digit.

$$\Gamma_{ab} = \frac{1}{8}(3 + 4\delta_{ab} + \cos\xi_{ab}) + \frac{\alpha}{2} k_{ab} \ln k_{ab}$$

$$k_{ab} = (1 - \cos\xi_{ab})/2$$

ST: $\alpha = 0$; **TT:** $\alpha = 3$

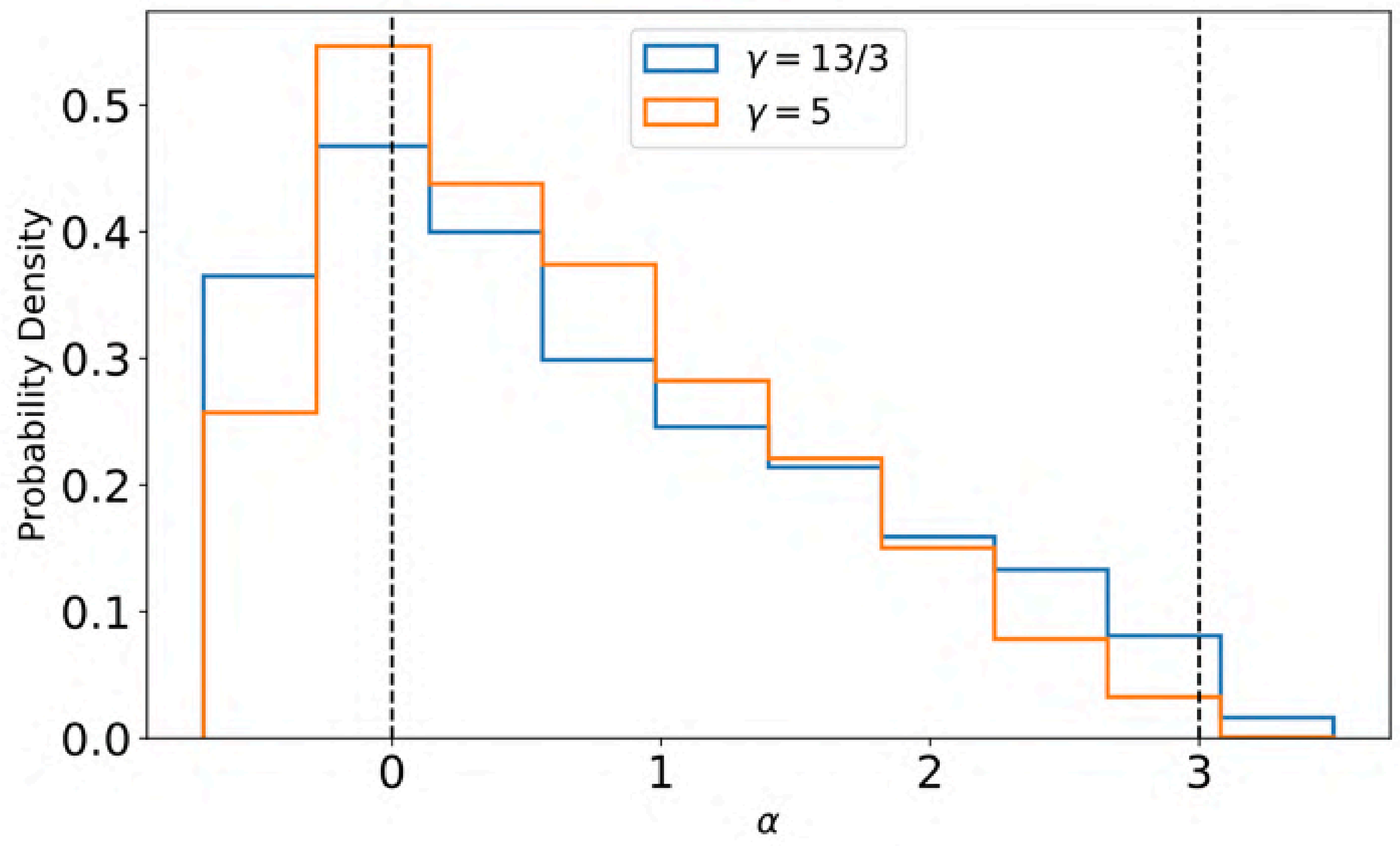

Chen, Wu & QGH, arXiv:2109.00296

The NANOGrav 12.5-year data set: Search for Non-Einsteinian Polarization Modes in the Gravitational-Wave Background

ZAVEN ARZOUMANIAN,[1] PAUL T. BAKER,[2] HARSHA BLUMER,[3,4] BENCE BÉCSY,[5] ADAM BRAZIER,[6,7] PAUL R. BROOK,[3,4]

ABSTRACT

We search NANOGrav's 12.5-year data set for evidence of a gravitational wave background (GWB) with all the spatial correlations allowed by general metric theories of gravity. We find no substantial evidence in favor of the existence of such correlations in our data. We find that scalar-transverse (ST) correlations yield signal-to-noise ratios and Bayes factors that are higher than quadrupolar (tensor transverse, TT) correlations. Specifically, we find ST correlations with a signal-to-noise ratio of 2.8 that are preferred over TT correlations (Hellings and Downs correlations) with Bayesian odds of about 20:1. However, the significance of ST correlations is reduced dramatically when we include modeling of the Solar System ephemeris systematics and/or remove pulsar J0030+0451 entirely from consideration. Even taking the nominal signal-to-noise ratios at face value, analyses of simulated data sets show that such values are not extremely unlikely to be observed in cases where only the usual TT modes are present in the GWB. In the absence of a detection of any polarization mode of gravity, we place upper limits on their amplitudes for a spectral index of $\gamma = 5$ and a reference frequency of $f_{\rm yr} = 1{\rm yr}^{-1}$. Among the upper limits for eight general families of metric theories of gravity, we find the values of $A^{95\%}_{TT} = (9.7 \pm 0.4) \times 10^{-16}$ and $A^{95\%}_{ST} = (1.4 \pm 0.03) \times 10^{-15}$ for the family of metric spacetime theories that contain both TT and ST modes.

Agree. (SNR<5)

Confirm our results in arXiv:2101.06869!

Longer observation is needed.

We do not yet understand why MSP J0030+0451 is causing this effect but we suspect incomplete noise modeling of this pulsar as the most plausible cause; MSP J0030+0451 has been shown to be problematic in detection analyses in the past (see Hazboun et al. 2020b). However, we do not believe that omitting MSP J0030+0451 from our analyses is the right solution to this problem. Rather, a thorough investigation of MSP J0030+0451's data, along with improved and more sophisticated noise modeling for this pulsar (and probably others) is the more robust path forward. NANOGrav is actively working on advanced noise modeling of the pulsars used in the 12.5-year data set and the results of these efforts are in preparation.

NANOGrav Collaboration, arXiv:2109.14706 of Eq. (25) with a Bayes factor greater than 100. Additionally, as a cross-check, we have reproduced the results of Chen et al. (2021), where a model with ST correlations with a spectral index of 5, [ST]M3A[5], was compared to a model without correlations and a spectral index of 13/3, M2A[13/3]. We obtain a Bayes factor of

With the release of a new data set on the horizon, NANOGrav's 15 year data set, we will continue to search for evidence of additional polarization modes of gravity. We anticipate that more pulsars, longer observation times, and improved noise modeling of pulsars will aid us greatly in finding and distinguishing the spatial correlation patterns in our data.

NANOGrav Collaboration, arXiv:2109.14706

Did LIGO/Virgo detect Primordial Black Holes?

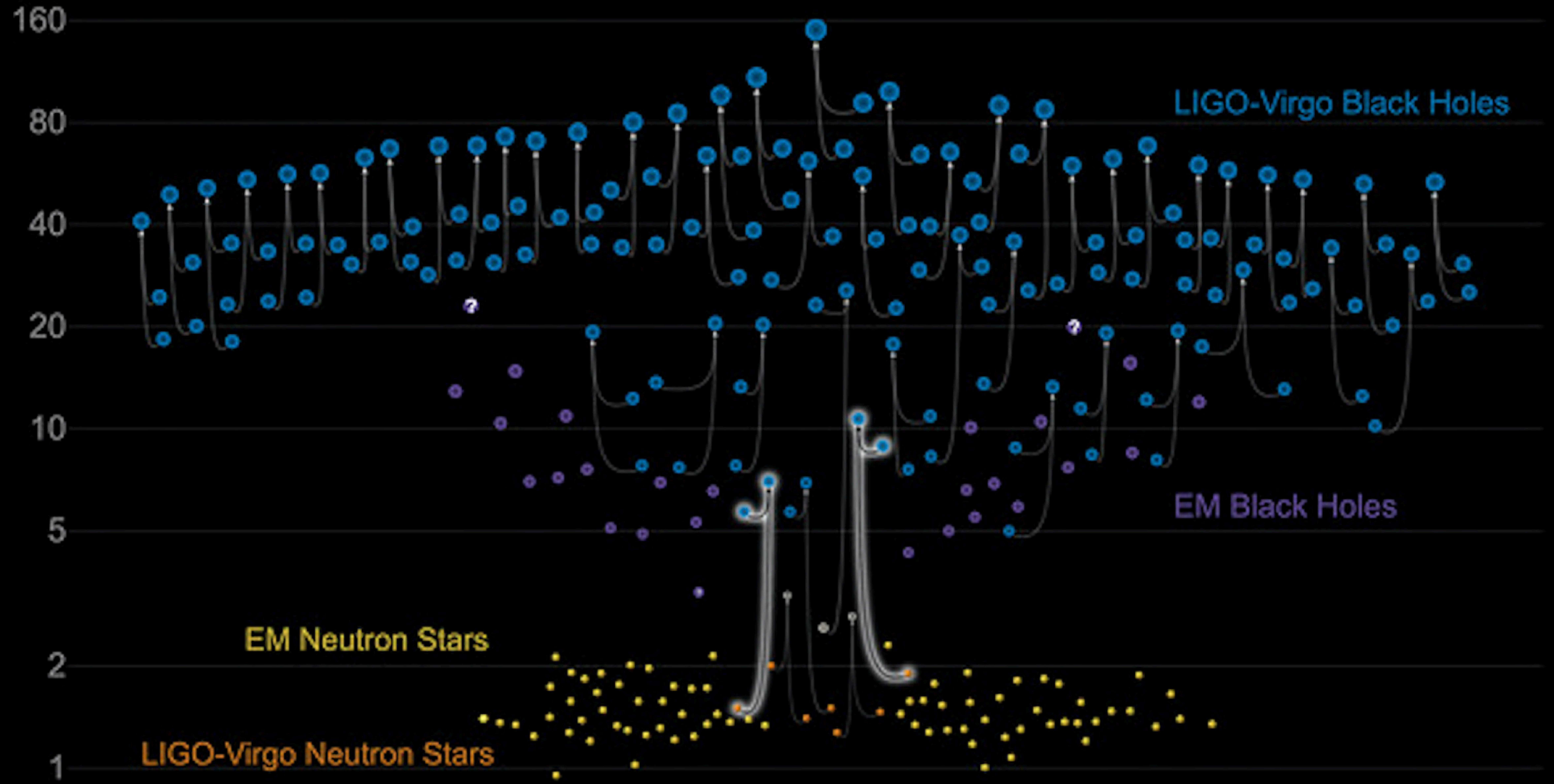

GW190521

(P)BH/mass gap?

The primary component of GW190521 has a high probability to be within the pair-instability supernovae mass gap, implying that the primary black hole might not have stellar origin.

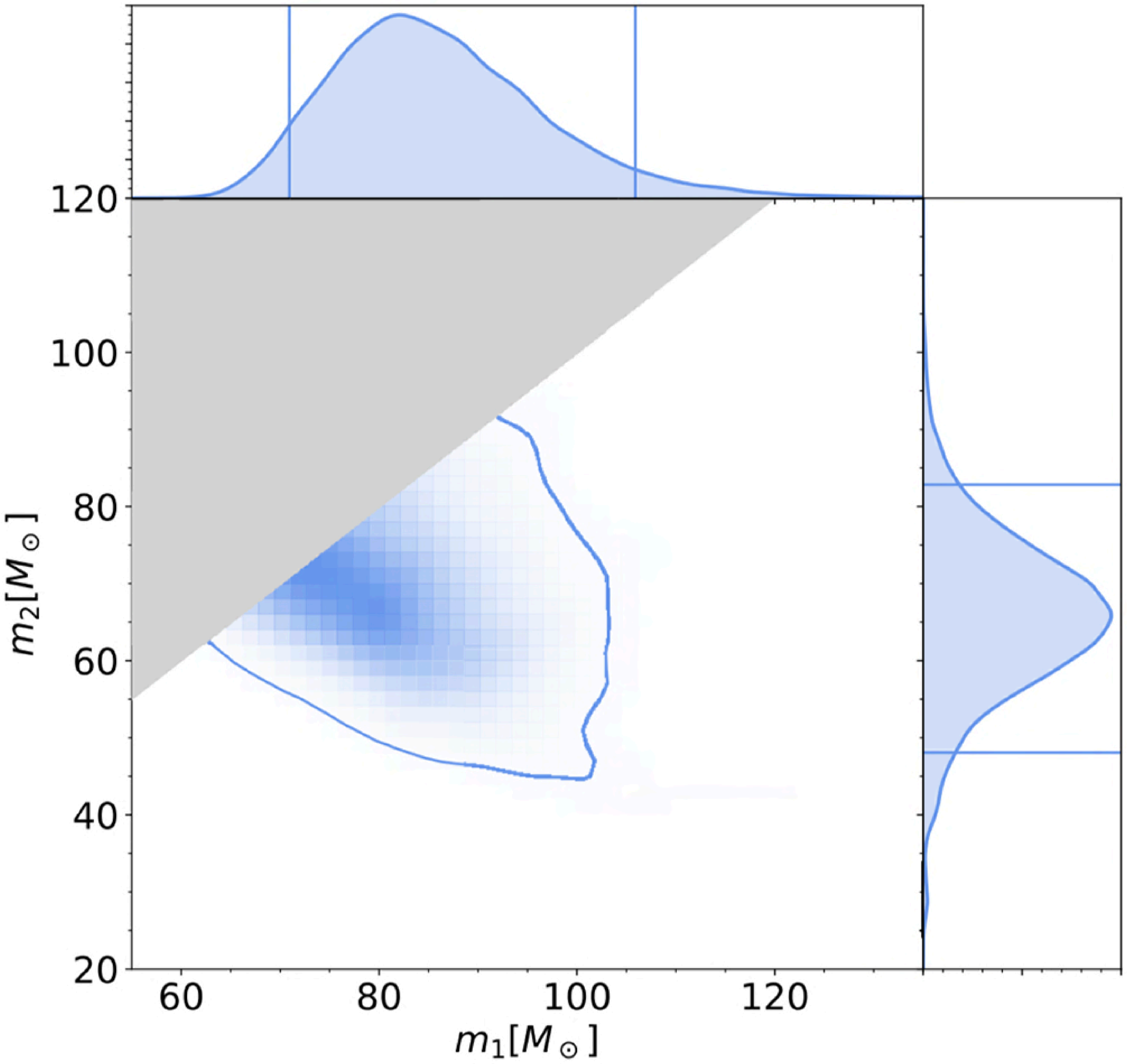

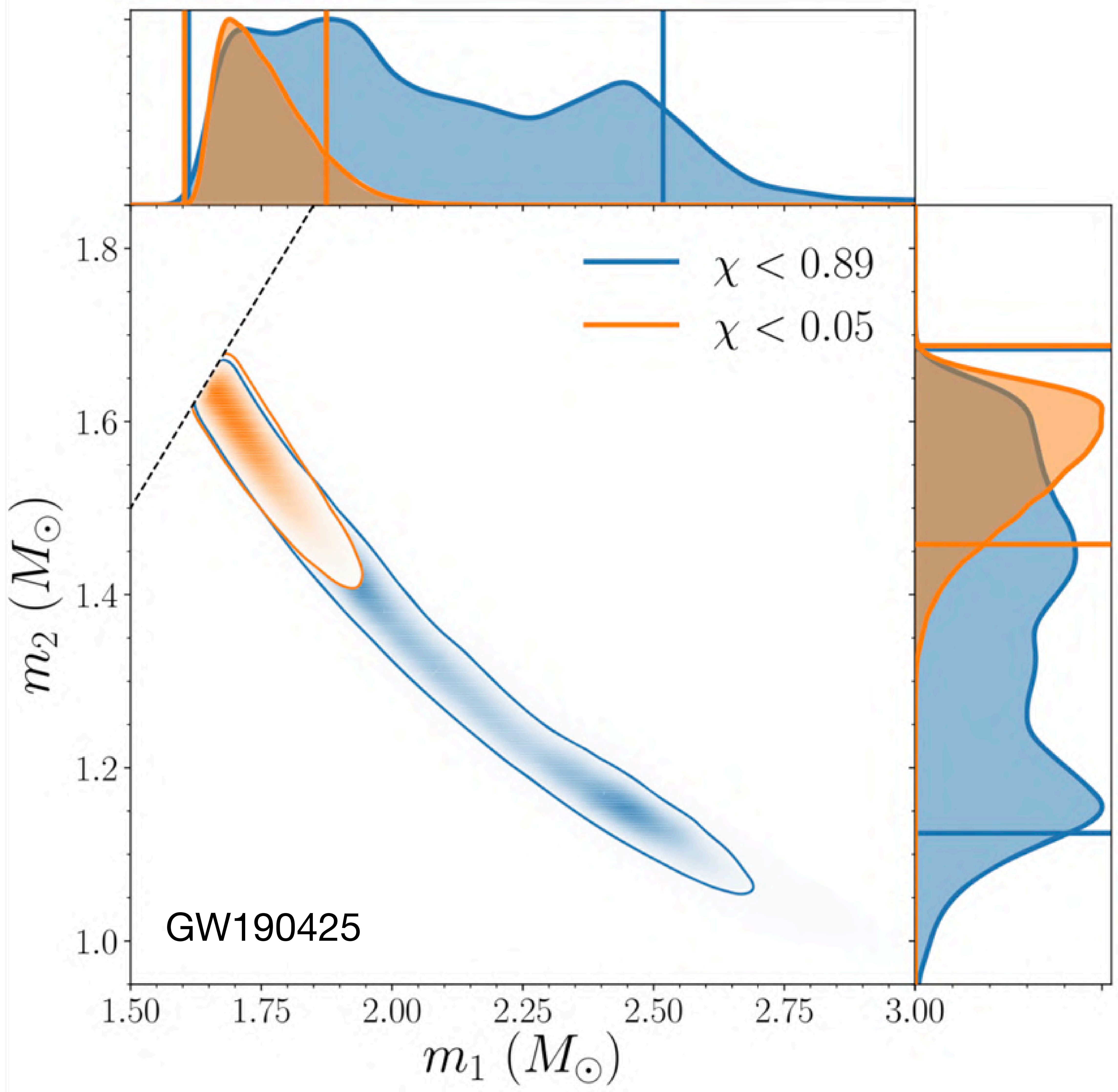

NS-NS/PBH-PBH?

Even though the component masses of GW190425 lie in the mass range of [1.12,2.52] solar mass and are consistent with the individual binary component being neutron star, the source-frame chirp mass and total mass are significantly larger than any known binary neutron star system.

GW190814 is reported to have a compact object with a mass of 2.5-2.67 solar mass, which falls in the lower mass gap where not neutron stars and black holes have been observed in a double compact-object system.

Even though the secondary component masses of GW200105 and GW200115 are well below the maximal mass of a neutron star, there are no electromagnetic counterparts to confirm.

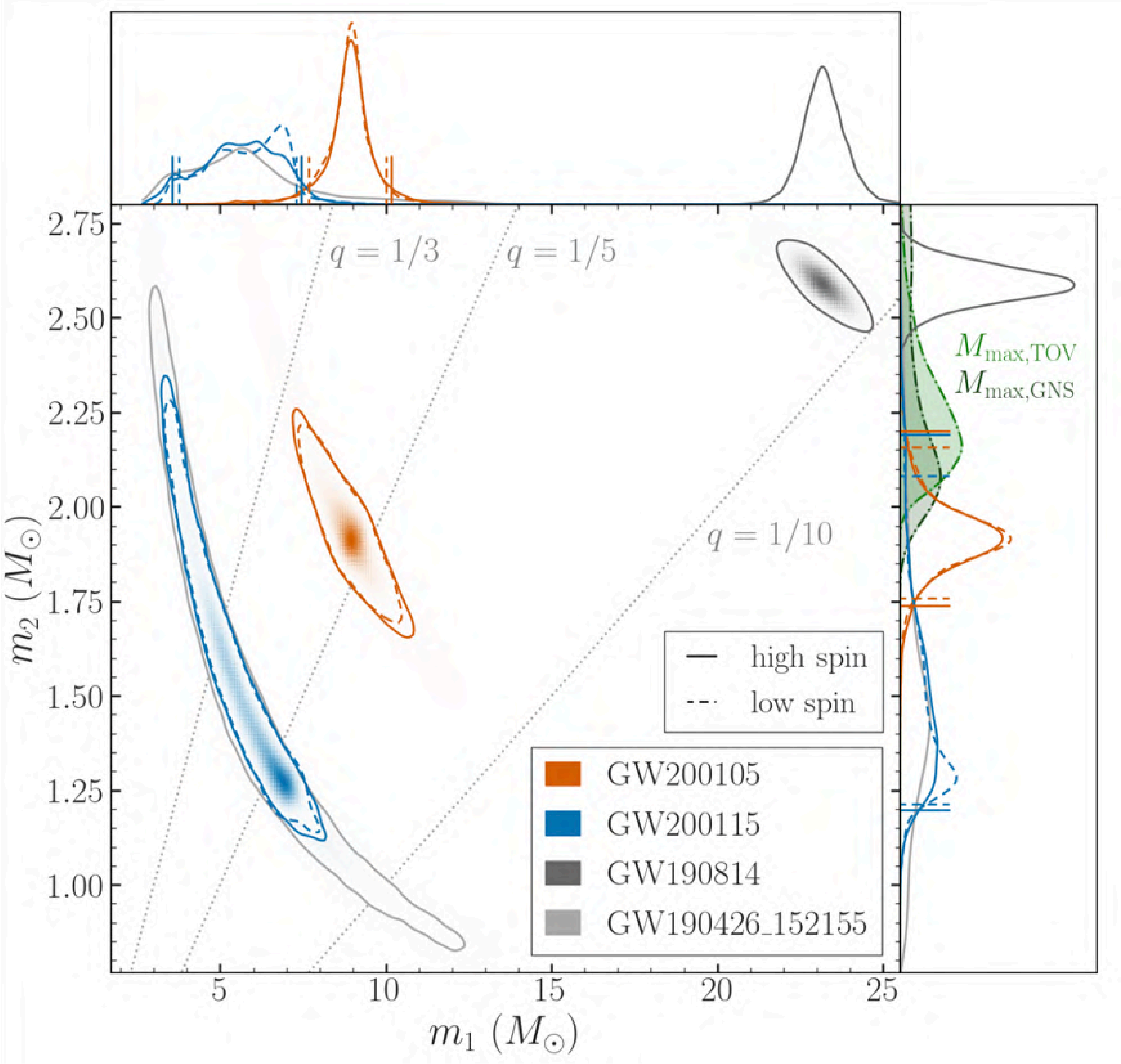

NS-BH/PBH-PBH?

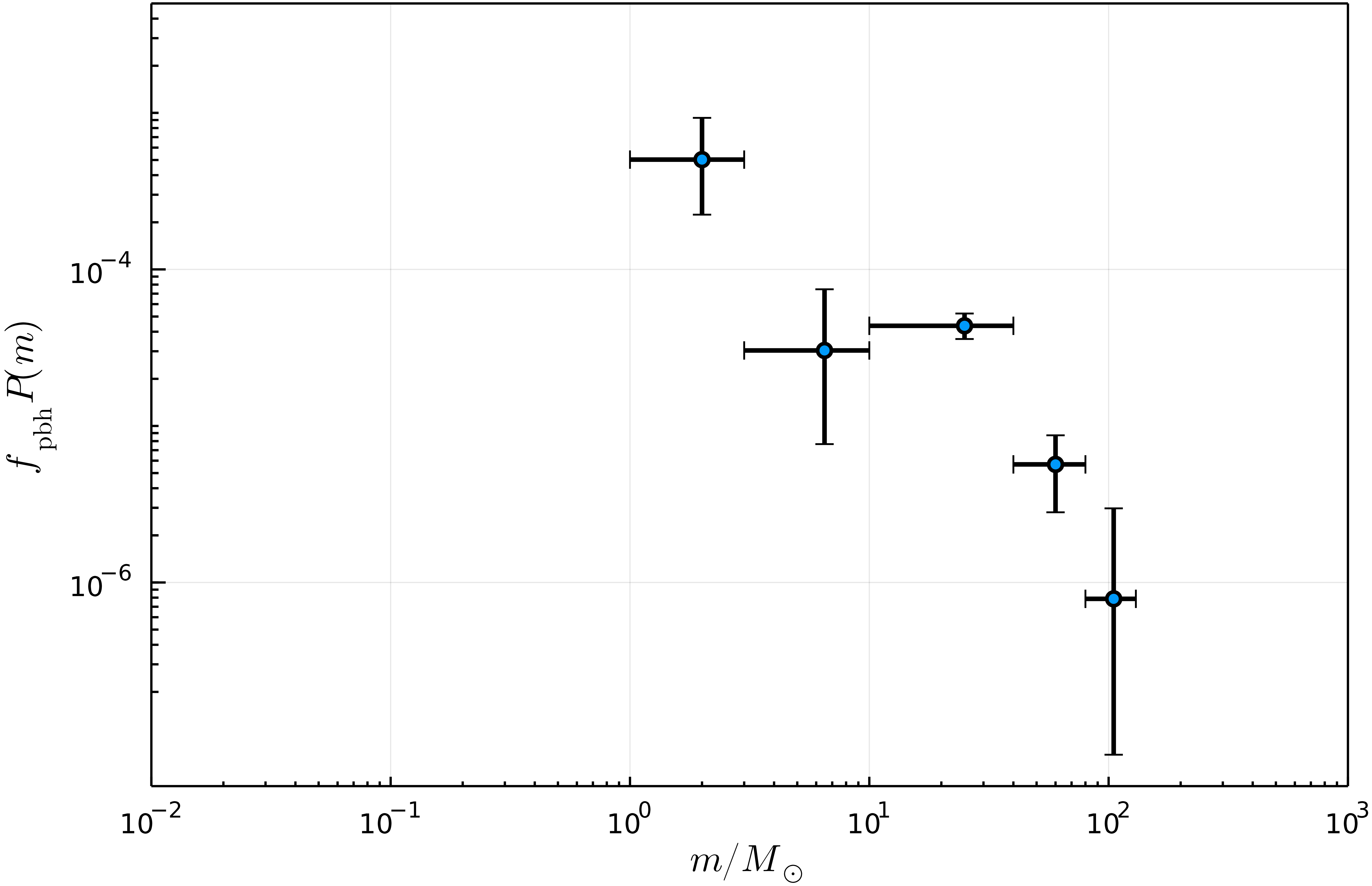

Our binned reconstruction of PBH mass function by adopting the GW events from GWTC-2 discarding events with false alarm rate larger than 1/yr and events with the the secondary component mass smaller than $3M_\odot$ to avoid contamination from putative events involving neutron stars, and also events with non-vanishing effective spin because the spin of PBHs is expected to be negligible at formation.

Chen, Yuan & QGH, arXiv:2108.11740

Event	R_{LVC} $\left[\text{Gpc}^{-3}\ \text{yr}^{-1}\right]$	R_{PBH} $\left[\text{Gpc}^{-3}\ \text{yr}^{-1}\right]$
GW190521	$0.13^{+0.30}_{-0.11}$	$0.12^{+0.15}_{-0.08}$ ✓
GW190425	460^{+1050}_{-390}	$1.0^{+2.0}_{-0.8}$ ✗
GW190814	7^{+16}_{-6}	$0.07^{+0.05}_{-0.04}$ ✗
GW200105	16^{+38}_{-14}	$0.9^{+1.3}_{-0.5}$ ✗
GW200115	36^{+82}_{-30}	$0.8^{+1.2}_{-0.5}$ ✗

Chen, Yuan & QGH, arXiv:2108.11740

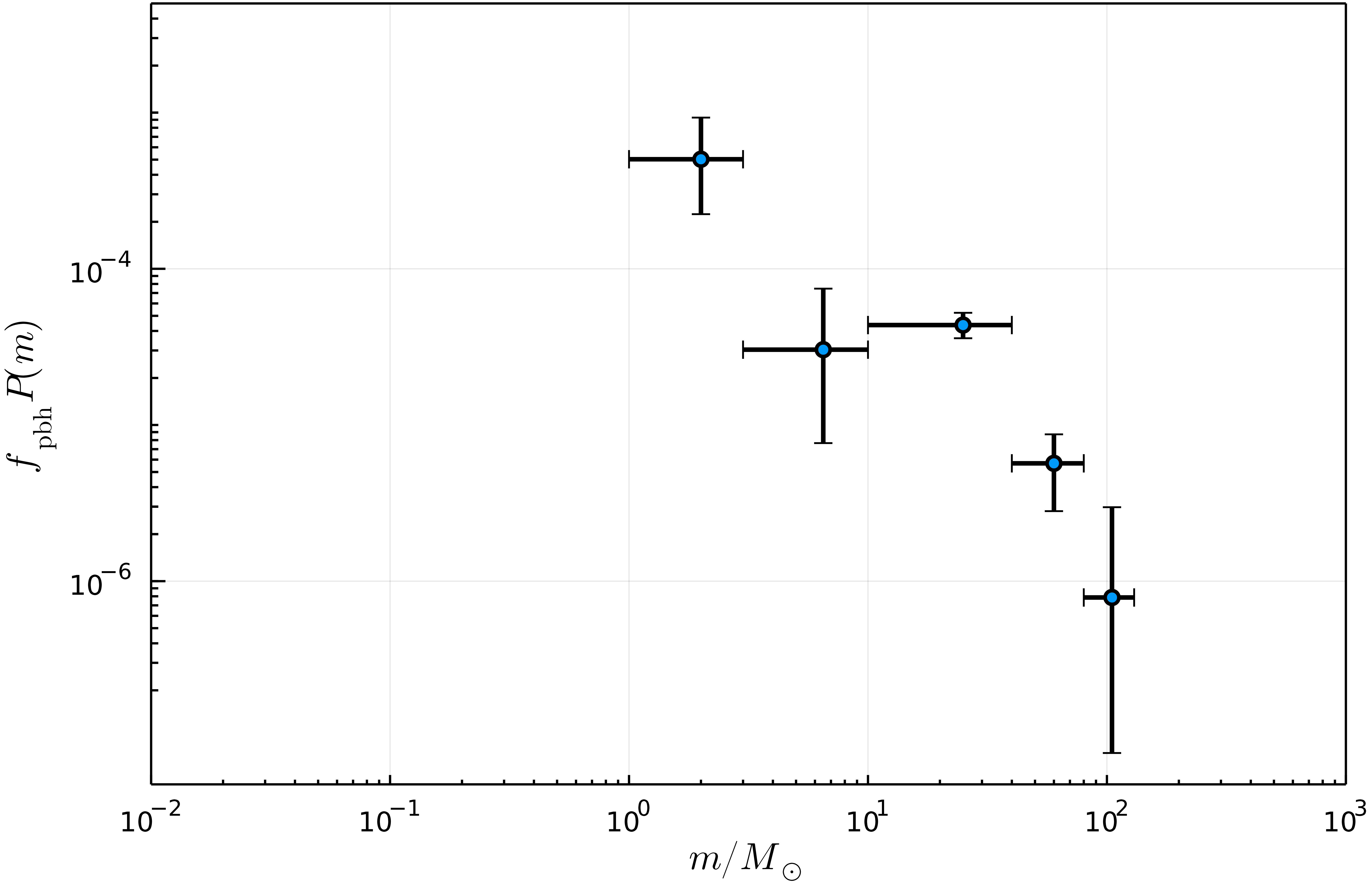

What is the physical origin of such a PBH mass function?

Chen, Yuan & QGH, arXiv:2108.11740

$$m_{pbh} \sim \mathcal{O}(10) M_\odot \;\Leftrightarrow\; t \sim 10^{-4} \textbf{ sec } [T \sim 10^2 \textbf{ Mev}]$$

QCD phase transition

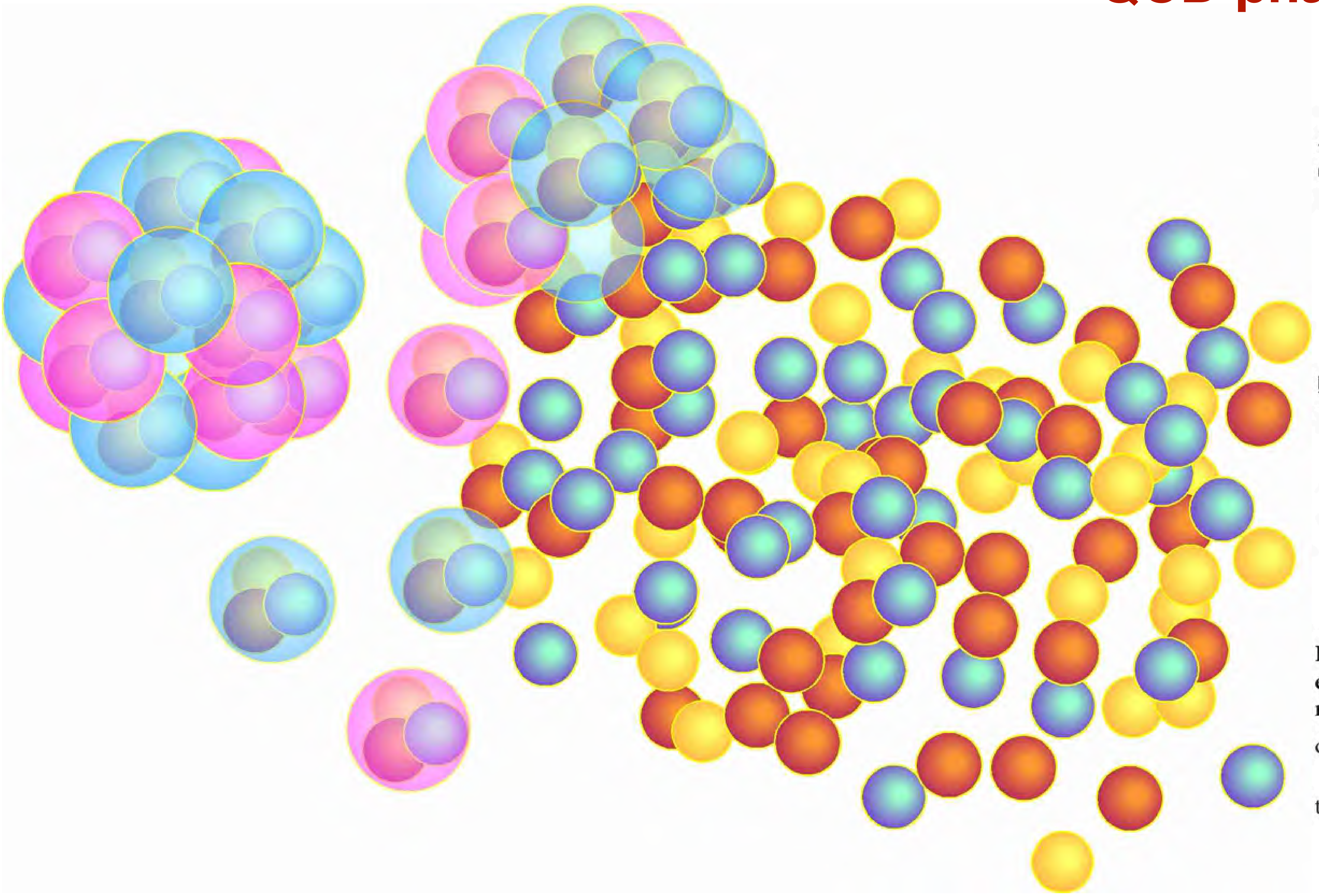

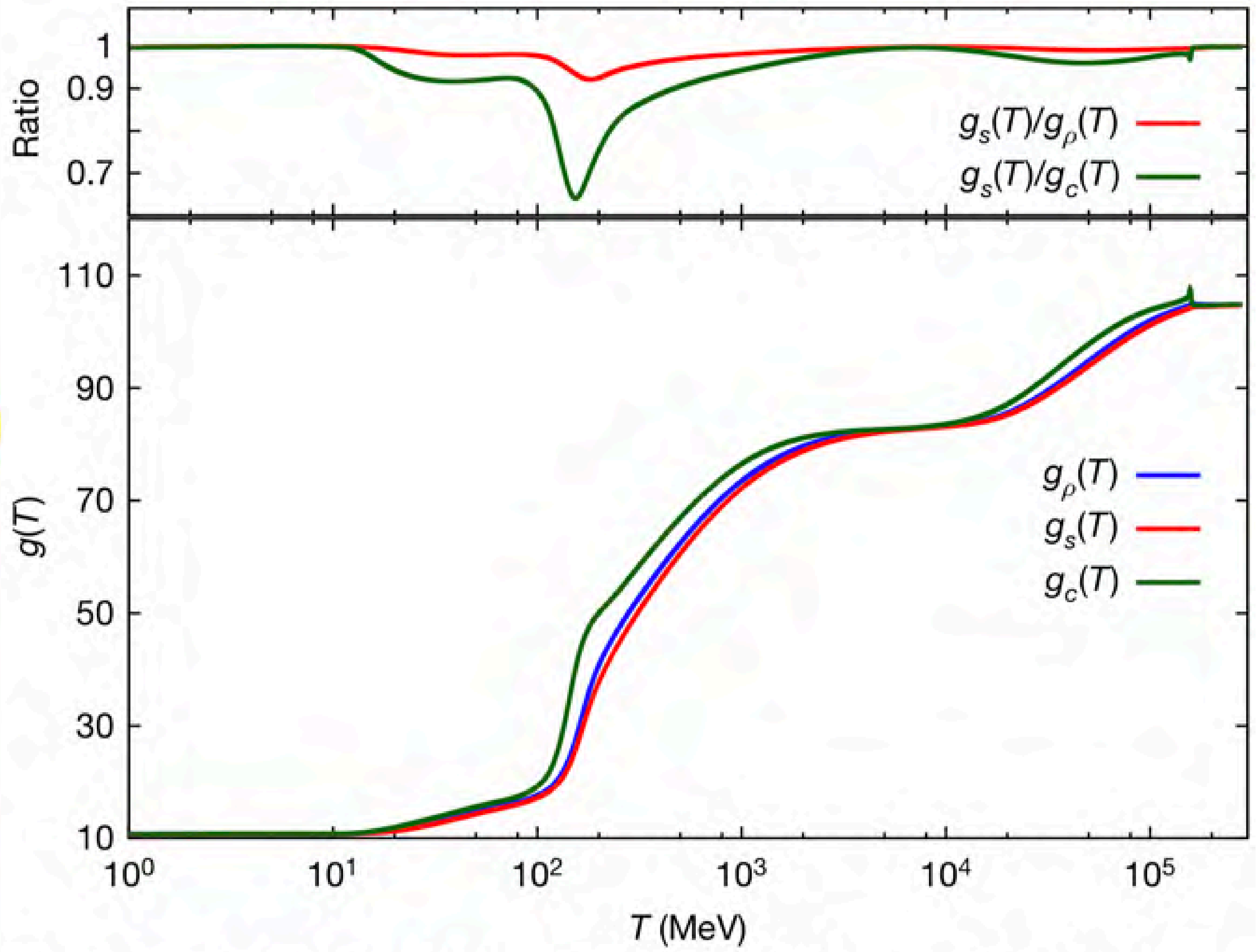

Figure 1 | The effective degrees of freedom of the energy density, the entropy density and the heat capacity in the early Universe, and their ratios. Shown as a function of temperature T in the lower panel are the degrees of freedom as follows: g_ρ for the energy density $\left(\rho = g_\rho \frac{\pi^2}{30} T^4\right)$, g_s for the entropy density $\left(s = g_s \frac{2\pi^2}{45} T^3\right)$, and g_c for the heat capacity $\left(c = g_c \frac{2\pi^2}{15} T^3\right)$.

Borsanyi et al., Nature (2016)

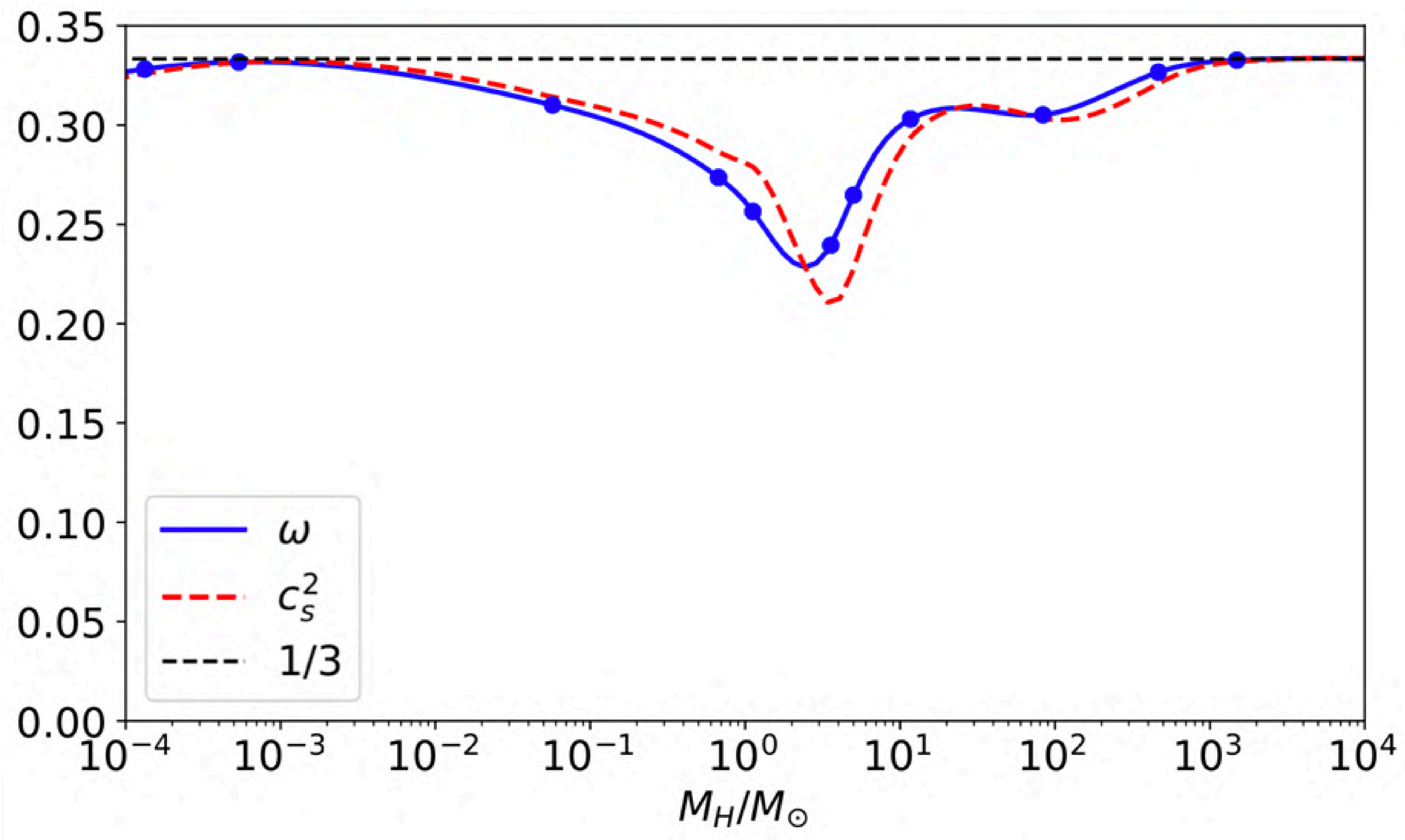

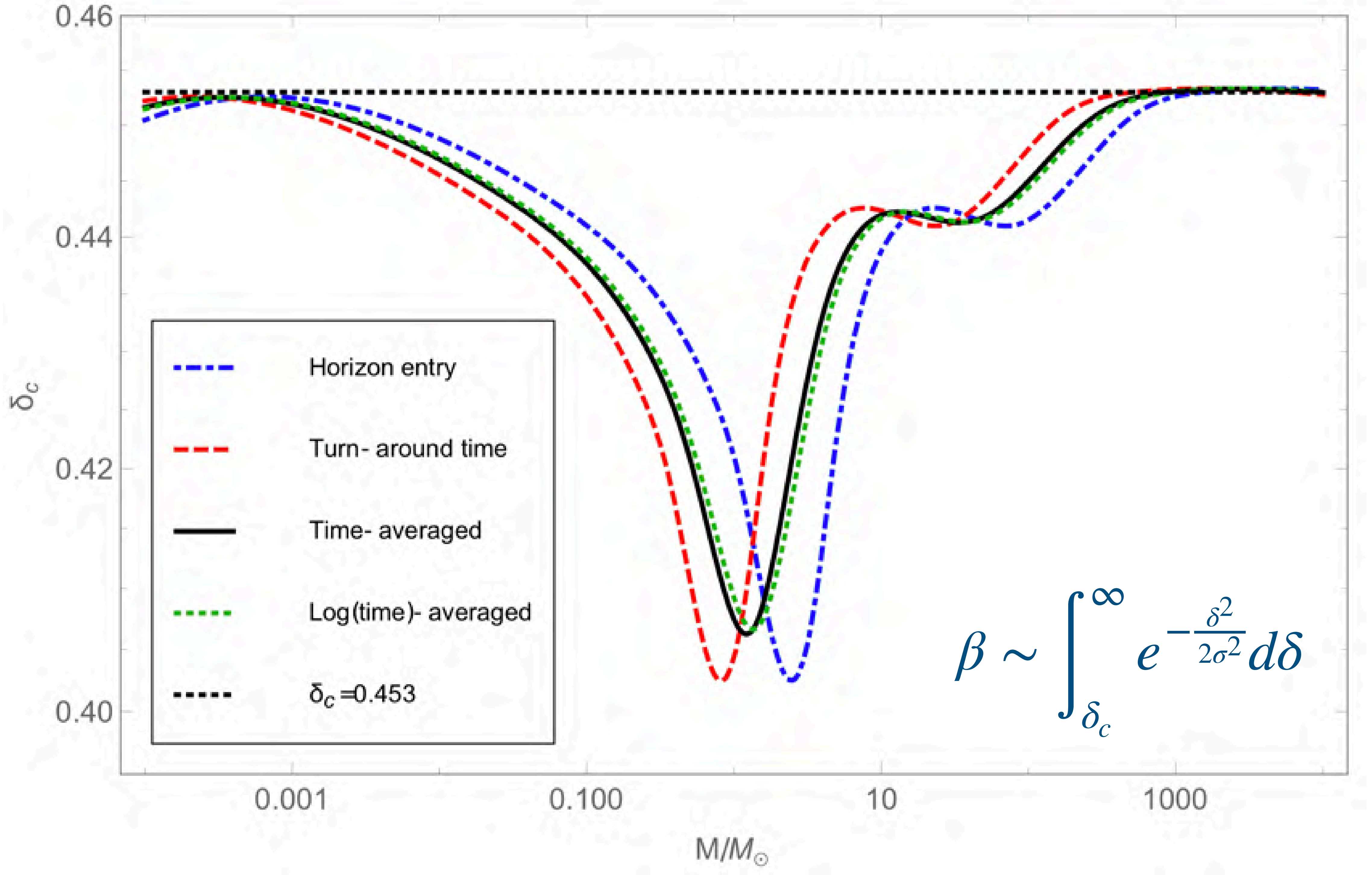

$$\beta \sim \int_{\delta_c}^{\infty} e^{-\frac{\delta^2}{2\sigma^2}} d\delta$$

$$w(T) = \frac{4g_s(T)}{3g_\rho(T)} - 1$$

$$c_s^2(T) = \frac{4(4g_s(T) + Tg_s'(T))}{3(4g_\rho(T) + Tg_\rho'(T))} - 1$$

The equation of state was soften during the QCD phase transition, and then the abundance of PBHs was enhanced.

Byrnes, Hindmarsh, Young, JCAP (2018)

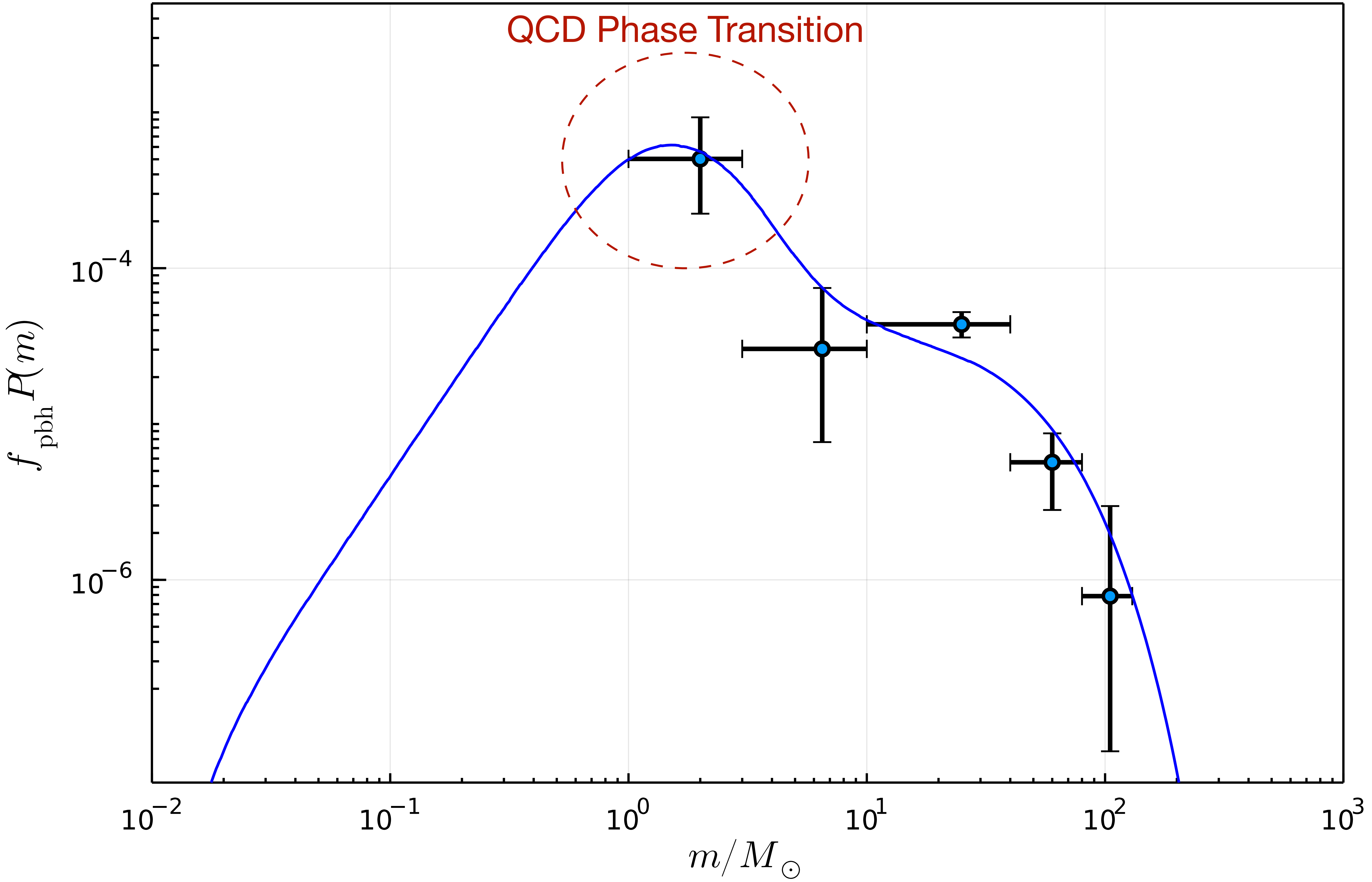

PBH mass function from a broad tilted curvature power spectrum

$$P_\zeta(k) = A(k/k_{min})^\alpha \times \Theta(k - k_{min})\Theta(k_{max} - k)$$

$A = 0.0047$

$\alpha = -0.11$

$k_{min} = 3.2 \times 10^5$ **Mpc**$^{-1}$

$k_{max} = 9.5 \times 10^6$ **Mpc**$^{-1}$

Chen, Yuan & QGH, arXiv:2108.11740

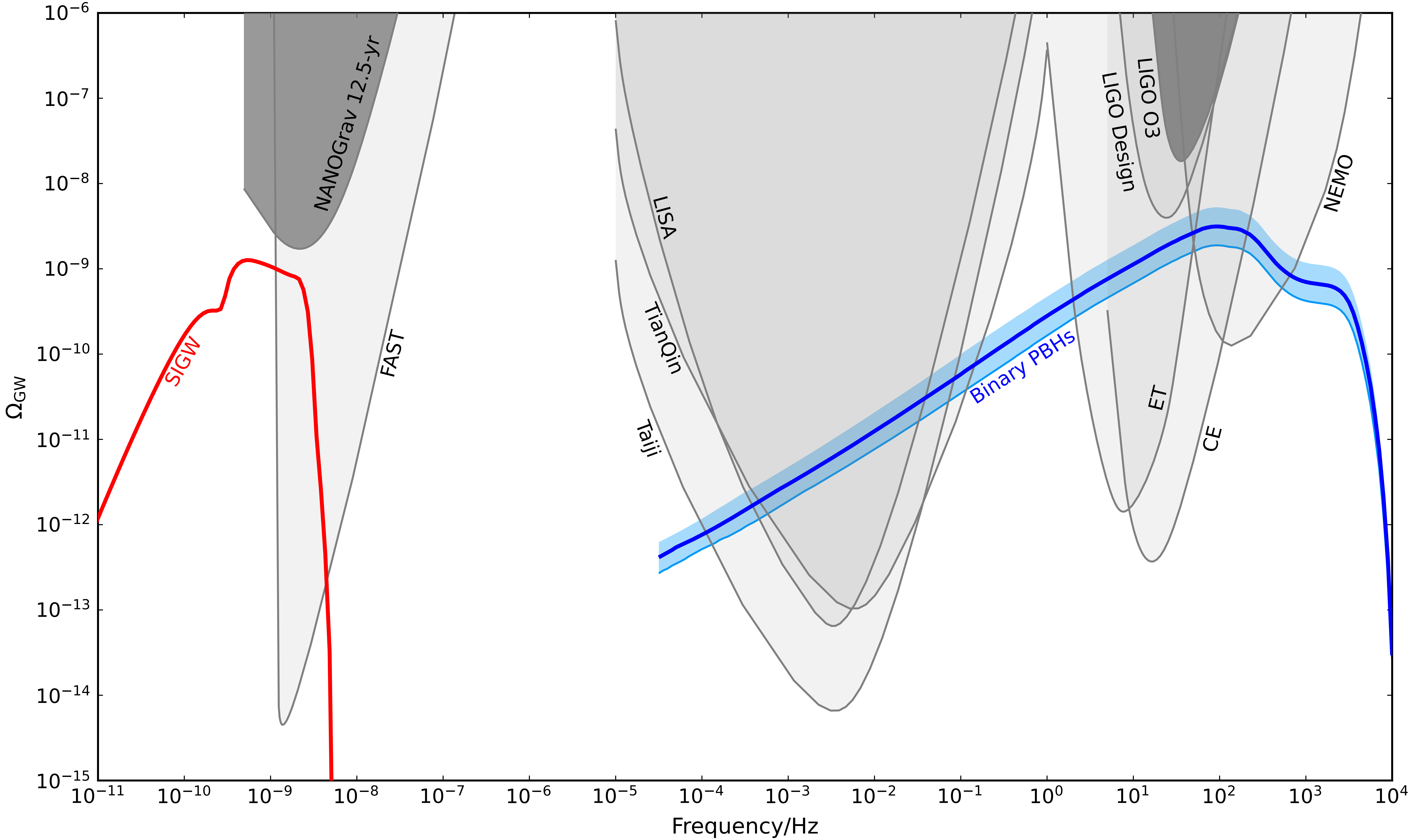

Chen, Yuan & QGH, arXiv:2108.11740

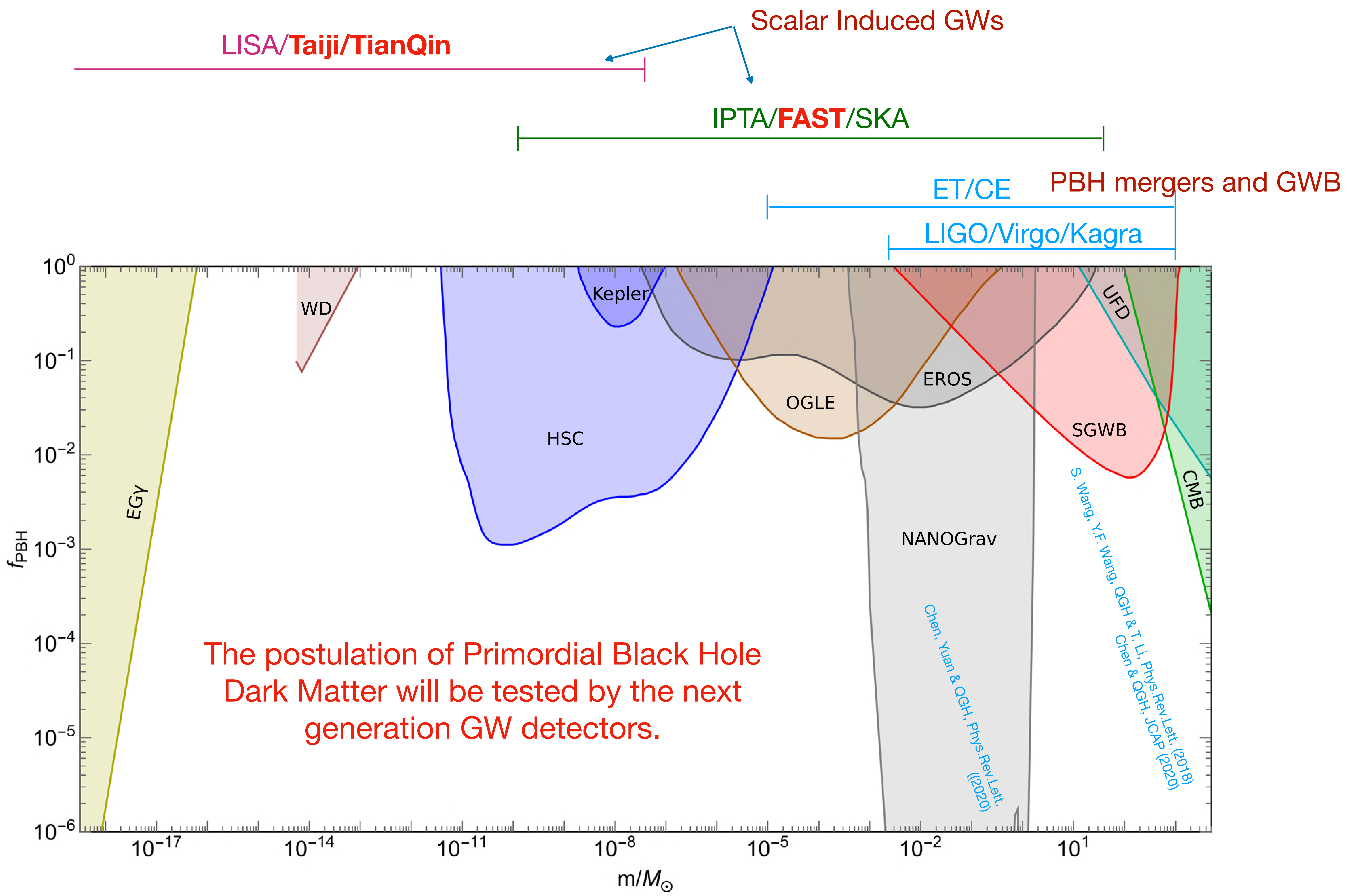

Scalar Induced GWs
LISA/Taiji/TianQin
IPTA/FAST/SKA
ET/CE
PBH mergers and GWB
LIGO/Virgo/Kagra
10^0
10^{-1}
10^{-2}
10^{-3}
10^{-4}
10^{-5}
10^{-6}
f_{PBH}
WD
Kepler
HSC
OGLE
EROS
UFD
SGWB
CMB
NANOGrav
EGγ
Chen, Yuan & QGH, Phys.Rev.Lett. (2020)
S. Wang, Y.F. Wang, QGH & T. Li, Phys.Rev.Lett. (2018)
Chen & QGH, JCAP (2020)
The postulation of Primordial Black Hole Dark Matter will be tested by the next generation GW detectors.
10^{-17}
10^{-14}
10^{-11}
10^{-8}
10^{-5}
10^{-2}
10^{1}
$m/M_{\odot}$

Thank you!